



## Design and synthesis of 7-O-1,2,3-triazole hesperetin derivatives to relieve inflammation of acute liver injury in mice



Yan Zheng<sup>a, b, c, d, 1</sup>, Yi-long Zhang<sup>a, c, d, 1</sup>, Zeng Li<sup>a, c, d</sup>, Wen Shi<sup>a, c, d</sup>, Ya-ru Ji<sup>a, c, d</sup>,  
Ya-Hui Guo<sup>a, c</sup>, Cheng Huang<sup>a, c, d</sup>, Guo-ping Sun<sup>b, c, \*\*</sup>, Jun Li<sup>a, c, d, \*</sup>

<sup>a</sup> Inflammation and Immune Mediated Diseases Laboratory of Anhui Province, Anhui Institute of Innovative Drugs, School of Pharmacy, Anhui Medical University, Hefei, 230032, China

<sup>b</sup> Department of Oncology, The First Affiliated Hospital of Anhui Medical University, Anhui Medical University, Hefei, 230032, Anhui, China

<sup>c</sup> Institute for Liver Diseases of Anhui Medical University, Anhui Medical University, Hefei, 230032, China

<sup>d</sup> The Key Laboratory of Anti-inflammatory of Immune Medicines, Ministry of Education, Hefei, 230032, China

### ARTICLE INFO

#### Article history:

Received 2 August 2020

Received in revised form

30 December 2020

Accepted 2 January 2021

Available online 15 January 2021

#### Keywords:

Hesperetin

Synthesis

Triazole

Structure-activity relationships

Anti-inflammatory activity introduction

### ABSTRACT

Based on the previous research results of our research group, to further improve the anti-inflammatory activity of hesperetin, we substituted triazole at the 7-OH branch of hesperetin. We also evaluated the anti-inflammatory activity of 39 new hesperetin derivatives. All compounds showed inhibitory effects on nitric oxide (NO) and inflammatory factors in **lipopolysaccharide**-induced RAW264.7 cells. Compound **d5** showed a strong inhibitory effect on NO (half maximal inhibitory concentration =  $2.34 \pm 0.7 \mu\text{M}$ ) and tumor necrosis factor- $\alpha$ , interleukin (IL)-1 $\beta$ , and (IL-6). Structure-activity relationships indicate that 7-O-triazole is buried in a medium-sized hydrophobic cavity that binds to the receptor. Compound **d5** can also reduce the reactive oxygen species production and significantly inhibit the expression of inducible NO synthase and cyclooxygenase-2 through the nuclear factor- $\kappa\text{B}$  signaling pathway. In vivo results indicate that **d5** can reduce liver inflammation in mice with acute liver injury (ALI) induced by  $\text{CCl}_4$ . In conclusion, **d5** may be a candidate drug for treating inflammation associated with ALI.

© 2021 Elsevier Masson SAS. All rights reserved.

## 1. Introduction

Acute liver injury (ALI) involves emergent hepatocellular damage accompanied by abnormal liver function [1,2]. ALI is usually associated with drug poisoning [3–5], viral hepatitis [6], immunological etiologies [7], chemical damage [8], and liver ischemia reperfusion. Drug-induced liver injury is the main cause of ALI and acute liver failure [9,10]. Most patients with ALI can recover through treatment, but others may progress to acute liver failure, which lacks effective treatment, with high mortality [7]. ALI is also closely related to the occurrence of fibrosis, cirrhosis, and hepatocellular carcinoma [4]. Therefore, seeking an effective treatment strategy is important.

Traditional Chinese medicine plays an important role in the treatment of ALI [11,12]. The traditional Chinese medicine tangerine peel has liver protection and anti-inflammatory pharmacological action in widespread clinical applications. Hesperetin and hesperidin, the main active ingredients of Chinese medicine orange peel, are isolated from dried tangerine or orange peel and belong to flavonoid compounds [13,14]. Flavonoids form anti-oxidant components, scavenge reactive oxygen species (ROS) [15], remove inflammation-mediated release of ALI inflammatory mediators, and inhibit liver fibrosis [16,17] and abnormal hepatocyte apoptosis [18,19]. Hesperetin is a flavonoid compound that has various pharmacological effects, including anti-inflammatory, anti-oxidation, and anti-tumor activities. Its anti-inflammatory activity is recognized and widely studied. However, given hesperetin's structural characteristics, its plasma circulation time is short, and easy removal from the body limits its wide application [20–22].

Our research group has been devoted to the research of hesperetin to improve its biological activity [23–26]. In the earlier pharmacokinetics studies of hesperetin and its derivatives, the 7-OH component of hesperetin was rapidly metabolized into 7-O-

\* Corresponding author. School of Pharmacy, Anhui Medical University, 81 Meishan Road, Hefei, Anhui Province, 230032, China.

\*\* Corresponding author. Department of Oncology, The First Affiliated Hospital of Anhui Medical University, 218 Jixi Road, Hefei, 230022, Anhui Province, China.

E-mail addresses: [sungp@ahmu.edu.cn](mailto:sungp@ahmu.edu.cn) (G.-p. Sun), [lj@ahmu.edu.cn](mailto:lj@ahmu.edu.cn) (J. Li).

<sup>1</sup> They contribute equally to this work.

sulfates and 7-O-glucuronides by phase II metabolism in the liver (Fig. 1) [22,27]. To improve the anti-inflammatory activity of hesperetin while reducing its elimination rate, we synthesized 23 new hesperetin derivatives in four series and evaluated their anti-inflammatory activity in vitro and in vivo [26]. In the primary analysis of the structure–activity relationships (SARs), the 7-O-substituent was the lipophilic region. Subsequently, we optimized 7-O-substituent hesperetin derivatives by amide substitution at 7-OH [25]. Studies of the 7-O-amide series of substituents further demonstrated that increasing the hydrophobicity of the side chains increased the anti-inflammatory activity of the derivatives, e.g. (6b (piperidine ethanol) < 6a (piperidine)). And the size of the amide side chain was appropriately increased, and its anti-inflammatory

activity was increased (4a (methyl) < 4b (ethyl) < 4d (propyl); 4j (cyclopropyl) < 4k (cyclopentyl)). Further, over-increasing the size of the side chain group would reduce the anti-inflammatory activity of the derivative, suggesting that the hydrophobic cavity was of medium size (4d (propyl) > 4f (butyl). 4k (cyclopentyl) > 4L (cyclohexyl)). The anti-inflammatory activities of 7-O-amide hesperetin derivatives increased significantly, with compounds **4d** and **4k** being the most effective with half maximal inhibitory concentrations (IC<sub>50</sub>) of 19.32 and 16.63 μM, respectively. Based on the SARs, we optimized hesperetin derivatives using the following strategies (Fig. 1): 1) Modification of 7-O-amide by replacement with triazole: 1,2,3-Triazole was observed in a variety of bioactive molecules as an anti-inflammatory and a non-classical bioisostere

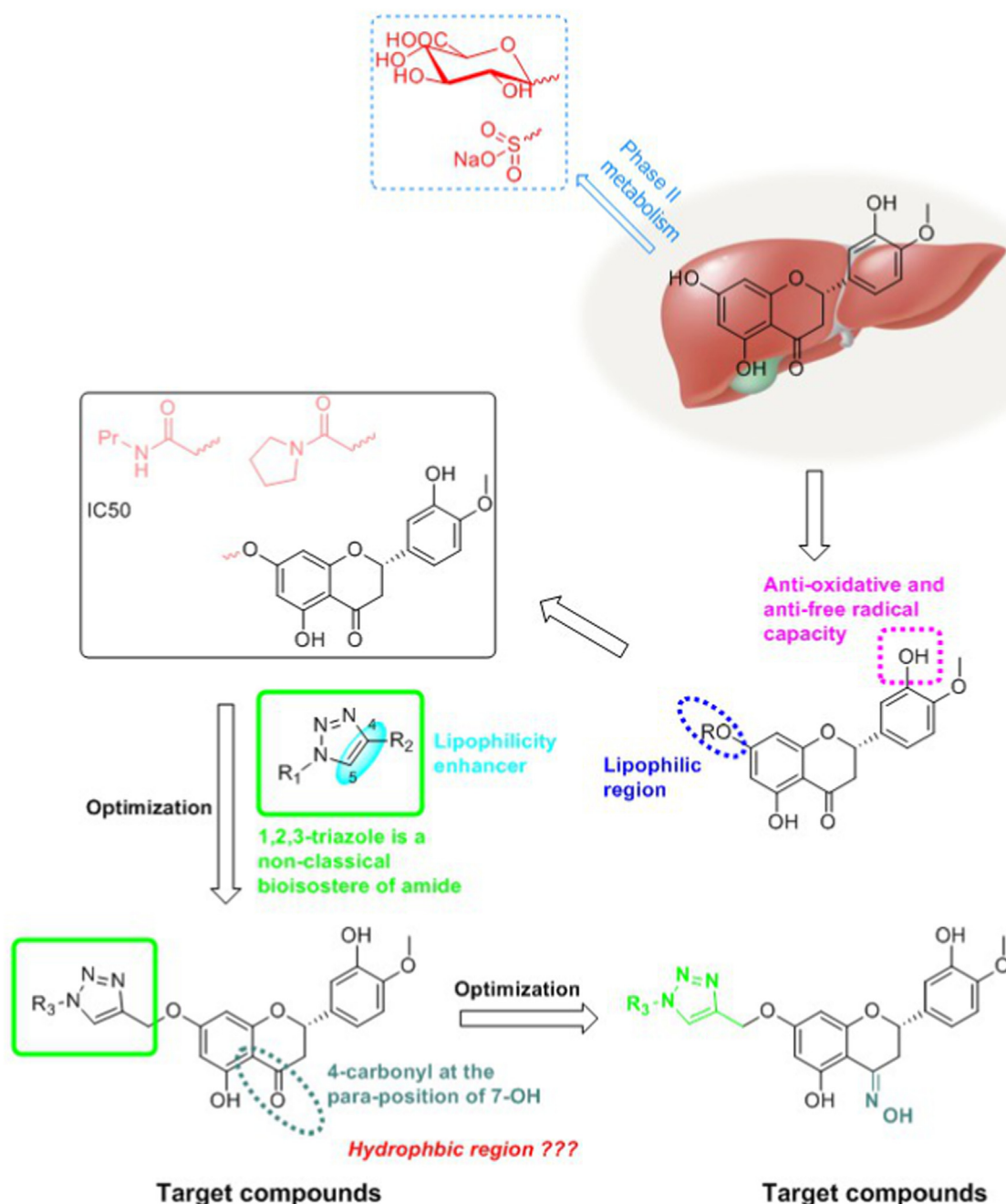


Fig. 1. Synthesized potent hesperetin derivatives along with their SARs for anti-inflammatory activity.

of amide. Enhance of lipophilicity with C<sub>4</sub> and C<sub>5</sub> of triazole: Triazole was more stable when metabolized than amide [28–33]. 2) Conversion of 4-carbonyl group to oxime: The 7-O-substituent was located in a hydrophobic region inside the binding pocket, in which the opposite 4-carbonyl group faces a hydrophilic region outside the binding pocket. We also converted the 4-carbonyl group into a more hydrophilic oximido; the converted form can significantly enhance the anti-inflammatory activity of the skeleton of various anti-inflammatory compounds [28,34,35]. We synthesized 39 hesperidin derivatives and evaluated their biological activity. Nearly all derivatives showed inhibitory effects on lipopolysaccharide (LPS)-induced nitric oxide (NO) release in RAW264.7 cells and decreased the production of tumor necrosis factor (TNF)- $\alpha$ , interleukin (IL)-1 $\beta$ , and (IL-6) inflammatory mediators. Derivative **d5** (IC<sub>50</sub> = 2.34  $\pm$  0.7  $\mu$ M) showed the best NO inhibitory activity and inflammatory factor inhibitory activity. We further analyzed the mechanism of action of **d5**. We also verified the remission effect of **d5** on inflammatory status in mice with ALI.

## 2. Results and discussion

### 2.1. Chemistry

As shown in Scheme 1, the target compounds **a1–a14**, **b1–b5**, **c1–c11**, and **d1–d9** were prepared following a straightforward synthesis starting with the hydrolysis of hesperidin. Hesperetin (**1**) was obtained by sulfuric acid hydrolysis of hesperidin in ethanol and then the synthesis of the target intermediate [36]. The resulting hesperetin was substituted by bromopropyne with K<sub>2</sub>CO<sub>3</sub> to obtain

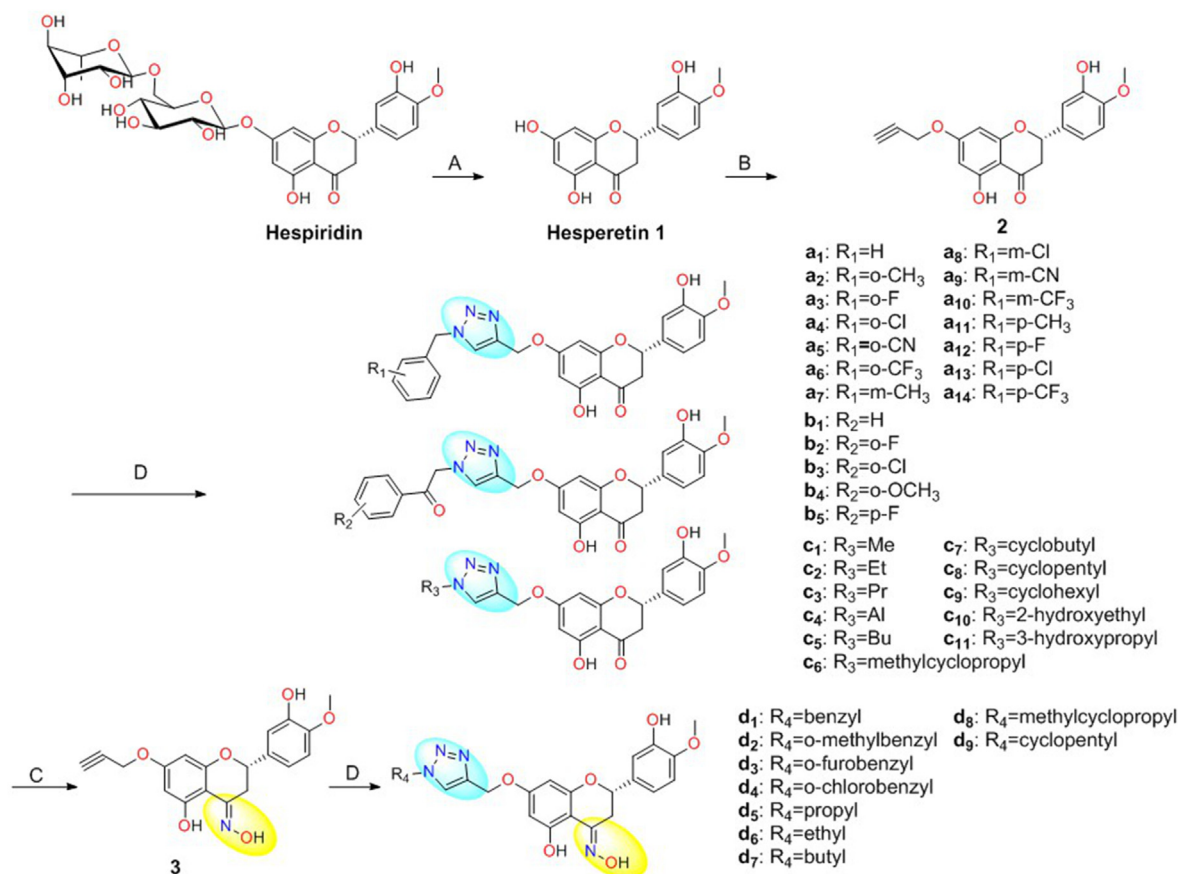
intermediate **2**. Intermediate **3** was obtained through the condensation reaction of intermediate **2** with hydroxylamine hydrochloride [34]. The methodology for the synthesis of target compounds was based on click chemistry catalyzed by monovalent copper ion employing intermediates **2** and **3** as precursors [31,33].

As shown in Table 1, for intermediate **2**, the chemical shift of 7-OH disappeared compared with hesperetin. Bromopropyne was selectively substituted at 7-OH. For intermediate **3**, the 5-OH shifted at 11.37 ppm, and the OH of oxime was at 11.43 ppm compared with that in intermediate **2** (proton nuclear magnetic resonance (<sup>1</sup>H NMR) spectra and chemical shifts of hesperidin are shown in Fig. S0 of Supporting Information).

### 2.2. Evaluation of biological activities in vitro

#### 2.2.1. Inhibitory activity of various compounds on NO

The production of NO, a pro-inflammatory mediator, is the key link to inflammation-related diseases. During inflammation, a large amount of NO is produced and further exacerbates the inflammatory response. Thus, inhibiting the production of NO can relieve or inhibit inflammatory diseases [37]. RAW 264.7 cells stimulated by LPS secrete pro-inflammatory mediators, such as NO, TNF- $\alpha$ , IL-1 $\beta$ , and IL-6, as a classic cell model for screening anti-inflammatory drugs. To detect the inhibitory effect of LPS-induced NO in RAW 264.7 cells by hesperetin derivatives, we used Griess reagent to detect the content of NO released by RAW264.7 cells after treatment with the compounds. As shown in Table 2, the content of NO in the untreated group was 0.5  $\pm$  0.4  $\mu$ M. After stimulation with LPS, compared with the untreated group, the content of NO in the



**Scheme 1.** Synthesis route of hesperetin derivatives **a1–a14**, **b1–b5**, **c1–c11**, and **d1–d9**. Conditions and reagents: (A) MeOH, 96% H<sub>2</sub>SO<sub>4</sub>, reflux; 80 °C. (B) K<sub>2</sub>CO<sub>3</sub>, propargyl bromide, dimethylformamide (DMF), r.t. (C) Ethanol, NH<sub>2</sub>OH·HCl, CH<sub>3</sub>COOK, 80 °C; reflux. (D) DMF, bromide, NaN<sub>3</sub>, r.t.; Vc, K<sub>2</sub>CO<sub>3</sub>, CuSO<sub>4</sub>·5H<sub>2</sub>O, r.t.

**Table 1**<sup>1</sup>H NMR data of OH of various compounds ( $\delta$  in ppm).

	5-OH	7-OH	3'-OH	N-OH
Hesperidin	12.03		9.10	
Hesperetin	12.14	10.80	9.11	
Intermediate 2	12.09		9.15	
Intermediate 3	11.37		9.10	11.43

**Table 2**NO concentration in LPS-treated RAW264.7 cells at a compound concentration of 10  $\mu$ M and IC<sub>50</sub> values.

Cmd	NO inhibition in 10 $\mu$ M (%)	IC <sub>50</sub> ( $\mu$ M)	Cmd	NO inhibition in 10 $\mu$ M (%)	IC <sub>50</sub> ( $\mu$ M)
<b>Ctrl</b>	0.5 $\pm$ 0.4 (NO content in cell supernatant)		<b>b4</b>	22.76 $\pm$ 9.43***	18.93 $\pm$ 2.07
<b>LPS</b>	30.19 $\pm$ 1.2 (NO content in cell supernatant)		<b>b5</b>	38.53 $\pm$ 10.8***	15.36 $\pm$ 2.63
<b>Hes</b>	18.36 $\pm$ 3.6***	48.59 $\pm$ 7.54	<b>c1</b>	39.99 $\pm$ 7.38***	15.24 $\pm$ 1.89
<b>4d</b>	35.23 $\pm$ 2.06***	20.89 $\pm$ 1.16	<b>c2</b>	41.4 $\pm$ 6.71***	15.03 $\pm$ 1.75
<b>4k</b>	38.68 $\pm$ 5.76***	19.14 $\pm$ 2.89	<b>c3</b>	56.39 $\pm$ 6.06***	9.67 $\pm$ 1.23
<b>a1</b>	49.8 $\pm$ 1.79***	10.95 $\pm$ 1.31	<b>c4</b>	50.06 $\pm$ 6.95***	13.82 $\pm$ 1.7
<b>a2</b>	45.69 $\pm$ 2.71***	13.08 $\pm$ 0.81	<b>c5</b>	49.89 $\pm$ 5.39***	13.9 $\pm$ 1.37
<b>a3</b>	63.34 $\pm$ 1.97***	7.32 $\pm$ 0.73	<b>c6</b>	48.78 $\pm$ 2.9***	11.88 $\pm$ 0.51
<b>a4</b>	63.14 $\pm$ 0.88***	6.14 $\pm$ 0.58	<b>c7</b>	44.16 $\pm$ 4.06***	15.31 $\pm$ 1.42
<b>a5</b>	43.59 $\pm$ 6.3***	14.61 $\pm$ 2.1	<b>c8</b>	53.82 $\pm$ 9.68***	10.52 $\pm$ 2.04
<b>a6</b>	48.04 $\pm$ 1.86***	12.49 $\pm$ 0.38	<b>c9</b>	42.37 $\pm$ 0.38***	15.61 $\pm$ 0.35
<b>a7</b>	30.96 $\pm$ 1.35***	17.42 $\pm$ 0.11	<b>c10</b>	24.73 $\pm$ 7.36***	17.75 $\pm$ 1.6
<b>a8</b>	28.04 $\pm$ 2.12***	18.23 $\pm$ 0.26	<b>c11</b>	32.75 $\pm$ 1.25***	16.74 $\pm$ 0.8
<b>a9</b>	32.9 $\pm$ 6.69***	17.99 $\pm$ 0.63	<b>d1</b>	63.65 $\pm$ 1.69***	6.13 $\pm$ 0.51
<b>a10</b>	35.53 $\pm$ 5.25***	19.87 $\pm$ 2.32	<b>d2</b>	22.53 $\pm$ 0.44***	18 $\pm$ 0.35
<b>a11</b>	29.42 $\pm$ 5.56***	16.84 $\pm$ 2.43	<b>d3</b>	65.36 $\pm$ 4.92***	5.71 $\pm$ 1.25
<b>a12</b>	41.42 $\pm$ 6.13***	15.09 $\pm$ 0.71	<b>d4</b>	33 $\pm$ 7.37***	13.35 $\pm$ 4.5
<b>a13</b>	28.99 $\pm$ 6.01***	17.76 $\pm$ 0.42	<b>d5</b>	67.47 $\pm$ 14.29***	2.34 $\pm$ 0.7
<b>a14</b>	36.44 $\pm$ 1.24***	17.73 $\pm$ 2.67	<b>d6</b>	65.13 $\pm$ 16.85***	3.14 $\pm$ 0.37
<b>b1</b>	32.15 $\pm$ 1.35***	16.89 $\pm$ 0.55	<b>d7</b>	56.91 $\pm$ 11.63***	8.9 $\pm$ 2.43
<b>b2</b>	34.46 $\pm$ 1.02***	18.91 $\pm$ 1.2	<b>d8</b>	67.03 $\pm$ 7.29***	6.32 $\pm$ 1.85
<b>b3</b>	34.07 $\pm$ 3.17***	13.19 $\pm$ 0.55	<b>d9</b>	63.71 $\pm$ 10.11***	6.88 $\pm$ 2.33

treatment group significantly increased to 30.19  $\pm$  1.26  $\mu$ M. Preliminary results showed that almost all compounds reduced the NO levels compared with the LPS stimulation group. Compounds **a3**, **a4**, **c3**, **c8**, **d1**, **d3**, **d5**, and **d6** significantly inhibited the production of NO induced by LPS. Hesperetin derivatives with triazole showed better NO inhibitory activity than those with amide, for example, **c3** (IC<sub>50</sub>: 9.67  $\pm$  1.23  $\mu$ M) > **4d** (IC<sub>50</sub>: 20.89  $\pm$  1.16  $\mu$ M); **c8** (IC<sub>50</sub>: 10.52  $\pm$  2.04  $\mu$ M) > **4k** (IC<sub>50</sub>: 19.14  $\pm$  2.89  $\mu$ M). The anti-inflammatory activities of 7-O-triazole hesperetin derivatives were twice better than that of 7-O-amide. Triazole increases hydrophobicity, thereby increasing their anti-inflammatory activities. Compounds with 4-oximido-7-O-triazole showed significantly improved activity compared with 7-O-triazole: **d5** (IC<sub>50</sub>: 2.34  $\pm$  0.7  $\mu$ M) > **c3** (IC<sub>50</sub>: 9.67  $\pm$  1.23  $\mu$ M); **d6** (IC<sub>50</sub>: 3.14  $\pm$  0.37  $\mu$ M) > **c2** (IC<sub>50</sub>: 15.03  $\pm$  1.75  $\mu$ M). The anti-inflammatory activities of 4-oximido-7-O-triazole hesperetin derivatives (**d5** and **d6**) were five times better than that of 7-O-triazole (**c3** and **c2**). Overall, 7-O-triazole and 4-oximido-7-O-triazole hesperetin derivatives exhibited better NO inhibitory activity than 7-O-amide.

Compound **d5** showed the best activity, which also reduced the production of NO in a concentration-dependent manner. Its inhibition rate was 67.47% at 10  $\mu$ M, and its IC<sub>50</sub> for NO inhibition was 2.34  $\pm$  0.7  $\mu$ M.

Table 2 shows the comparison of the inhibitory capability on NO of the compounds and the positive control drug at a concentration of 10  $\mu$ M VS LPS group. The test compounds (10  $\mu$ M) and positive drugs were 2 h before LPS stimulation. The data are presented as mean  $\pm$  standard deviation (SD) (n = 3). The difference was considered statistically significant when p (\*) < 0.05, (\*\*) < 0.01, (\*\*\*) < 0.001 vs LPS group.

### 2.2.2. Assessment of cytotoxicity

Methyl thiazolyl tetrazolium (MTT) assay was used to screen the non-cytotoxic dose of hesperetin derivatives in RAW264.7 cells [38]. Table 3 shows the results. Preliminary screening results showed that most of the compounds exhibited non-toxicity at 40  $\mu$ M. Thus, the effect of compound toxicity on cell viability was ruled out. The inhibitory activities displayed by compounds on

**Table 3**

Compound effects on RAW264.7 cell viability was evaluated at the compound concentration of 40  $\mu$ M.

Compound	%cell viability at 40 $\mu$ M	Compound	%cell viability at 40 $\mu$ M
Hes	1.21 $\pm$ 0.12***	b5	0.64 $\pm$ 0.03***
Ind	0.87 $\pm$ 0.08 <sup>ns</sup>	c1	1.05 $\pm$ 0.11 <sup>ns</sup>
Cel	0.83 $\pm$ 0.06 <sup>ns</sup>	c2	1.06 $\pm$ 0.11 <sup>ns</sup>
a1	0.98 $\pm$ 0.06 <sup>ns</sup>	c3	1.14 $\pm$ 0.11 <sup>ns</sup>
a2	1 $\pm$ 0.08 <sup>ns</sup>	c4	1.18 $\pm$ 0.1 <sup>ns</sup>
a3	0.74 $\pm$ 0.11***	c5	1.18 $\pm$ 0.06 <sup>ns</sup>
a4	0.83 $\pm$ 0.05 <sup>ns</sup>	c6	0.87 $\pm$ 0.07 <sup>ns</sup>
a5	1.14 $\pm$ 0.09 <sup>ns</sup>	c7	1.11 $\pm$ 0.09 <sup>ns</sup>
a6	1.35 $\pm$ 0.1***	c8	1.1 $\pm$ 0.08 <sup>ns</sup>
a7	1.13 $\pm$ 0.08 <sup>ns</sup>	c9	1.24 $\pm$ 0.12**
a8	1.2 $\pm$ 0.08*	c10	1.12 $\pm$ 0.08 <sup>ns</sup>
a9	0.56 $\pm$ 0.05***	c11	1.21 $\pm$ 0.04*
a10	0.93 $\pm$ 0.05 <sup>ns</sup>	d1	0.93 $\pm$ 0.02 <sup>ns</sup>
a11	1.1 $\pm$ 0.05 <sup>ns</sup>	d2	0.83 $\pm$ 0.03 <sup>ns</sup>
a12	1.01 $\pm$ 0.06 <sup>ns</sup>	d3	0.82 $\pm$ 0.07*
a13	0.94 $\pm$ 0.02 <sup>ns</sup>	d4	0.86 $\pm$ 0.04 <sup>ns</sup>
a14	0.66 $\pm$ 0.01***	d5	1.14 $\pm$ 0.04 <sup>ns</sup>
b1	1.12 $\pm$ 0.04 <sup>ns</sup>	d6	1.01 $\pm$ 0.08 <sup>ns</sup>
b2	1.13 $\pm$ 0.02 <sup>ns</sup>	d7	0.62 $\pm$ 0.03***
b3	0.99 $\pm$ 0.01 <sup>ns</sup>	d8	0.86 $\pm$ 0.03 <sup>ns</sup>
b4	1.32 $\pm$ 0.12***	d9	1.12 $\pm$ 0.07 <sup>ns</sup>

Results are the mean  $\pm$  SD of three experiments. The difference was considered statistically significant when p (\*) < 0.05, (\*\*) < 0.01, (\*\*\*) < 0.001, ns: no significance vs LPS group. Hes: hesperetin, Ind: indomethacin, Cel: celecoxib vs LPS group.

indicators, such as NO and inflammatory factors, were unaffected by compound toxicity. Thus, further study of the anti-inflammatory activities of the compounds should be set below 40  $\mu$ M.

Compound **d5** showed excellent inhibitory activity according to the results of NO inhibition activity. Thus, we compared the activity of compound **d5** at different concentrations on LPS-induced RAW264.7 cells in the LPS group. Compound **d5** showed no toxicity at 60  $\mu$ M. In addition, compared with the LPS group with the control, we observed that cells proliferated slightly after 24 h of LPS stimulation. The results are shown in Fig. 2.

### 2.2.3. Test compounds inhibit LPS-induced cytokine production in RAW264.7 cells

Multiple inflammatory factors, including TNF- $\alpha$ , IL-1 $\beta$ , and IL-6, are involved in and accelerate inflammatory responses during inflammatory progression [39]. Therefore, the effective suppression of inflammatory factors is considered an effective marker for the treatment of inflammation. The effects of compound action on TNF-

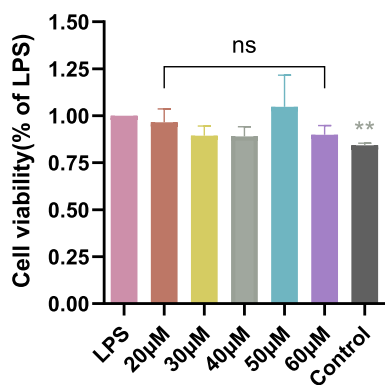


**Fig. 2.** Compound **d5** at different concentrations affected the viability of RAW264.7 cells compared with the LPS group. The results are the mean  $\pm$  SD of three experiments. The difference was considered statistically significant when p (\*) < 0.05, (\*\*) < 0.01, (\*\*\*) < 0.001, ns: no significance.

$\alpha$ , IL-1 $\beta$ , and IL-6 levels in LPS-stimulated supernatant of RAW264.7 cells were detected by enzyme-linked immunosorbent assay (ELISA). First, we initially evaluated the suppression effects of all compounds on LPS-induced RAW264.7 inflammatory response-related factors at a concentration of 10  $\mu$ M. Fig. 3A–C shows the results. Overall, compared with normal basal levels, LPS stimulation significantly increased the production of cytokines TNF- $\alpha$ , IL-1 $\beta$ , and IL-6 in macrophages. Overall, almost all newly synthesized triazole derivatives showed better inhibitory activities than hesperetin and the positive controls indomethacin and celecoxib. In addition, compared with amide derivatives in **4d** and **4k**, the newly synthesized triazole derivatives showed a significant improvement in the inhibitory capability for inflammatory factors. Compared with **b1–b5** and **c1–c11** series, **a1–a14** and **d1–d9** series showed better inhibitory effects. Combined with the MTT experiment, the compounds of **a1**, **a2**, and **a3** had a high inhibition rate against NO, but they exhibited strong cytotoxicity. Compared with the other series, the compounds of **d1–d9** had the best and extremely significant inhibitory capability on inflammatory factors, which were roughly the same as our previous NO measurement results. We also detected the inhibitory effect of different concentrations of **d5** (1.25, 2.5, 5, 10, and 20  $\mu$ M) on LPS-induced RAW264.7 inflammatory factors. Fig. 3D–F reveal the concentration-dependent inhibition of inflammatory factors by **d5**. Next, we selected compound **d5**, which showed the most effects, to explore the anti-inflammatory mechanism of the series derivatives.

### 2.2.4. Suppression effects of compound **d5** on the expression of cyclooxygenase-2 (COX-2) and induced NO synthase (iNOS) in RAW264.7 cells stimulated by LPS

In the inflammatory process, iNOS is overexpressed under the action of inflammatory cytokines, leading to NO overproduction [40]. Western blotting was used to analyze whether the inhibitory effects of compound **d5** on LPS-induced NO occur through the suppression effects on iNOS. The protein levels of iNOS were determined by LPS stimulation (1  $\mu$ g/mL) at different concentrations of **d5** (5, 10, and 20  $\mu$ M) for 24 h. As shown in Fig. 4, **d5** inhibited the expression of iNOS in RAW264.7 cells stimulated by LPS in a concentration-dependent manner. COX-2, as an important anti-inflammatory indicator, maintains a low expression level in normal tissues. COX-2 is up-regulated in the occurrence of inflammation, and prostaglandin secretion and other downstream inflammatory mediators are rapidly increased, further intensifying the disease's inflammatory process [41,42]. We also confirmed that compound **d5** reduced COX-2 expression in a concentration-dependent manner with Bay 11–7082 (5  $\mu$ M) as the positive control (Fig. 4).

### 2.2.5. Compound **d5** regulates the inflammatory effect on RAW264.7 cells by LPS stimulation through negatively regulating the nuclear factor (NF)- $\kappa$ B signaling pathway

NF- $\kappa$ B is a transcription factor known to regulate inflammation positively [43]. When LPS stimulates RAW264.7 cells to activate NF- $\kappa$ B, the activated NF- $\kappa$ B (I $\kappa$ B) protein phosphorylation releases NF- $\kappa$ B p65 subunits from it, transfers them to the nucleus, binds to the target promoter, and initiates transcription of inflammatory genes, including TNF- $\alpha$ , IL-1 $\beta$ , IL-6, iNOS, and COX-2 [44,45]. Western blotting was used to detect the effect of **d5** on the transcriptional activity of LPS-induced RAW264.7 cells.

As shown in Fig. 5, **d5** significantly reduced I $\kappa$ B $\alpha$  phosphorylation compared with the LPS induction group. At the same time, compound **d5** (5, 10, and 20  $\mu$ M) inhibited LPS-induced nuclear translocation of NF- $\kappa$ Bp65 in a concentration-dependent manner. The above results indicate that the anti-inflammatory effects of compound **d5** may be achieved through negative regulation of NF- $\kappa$ B.

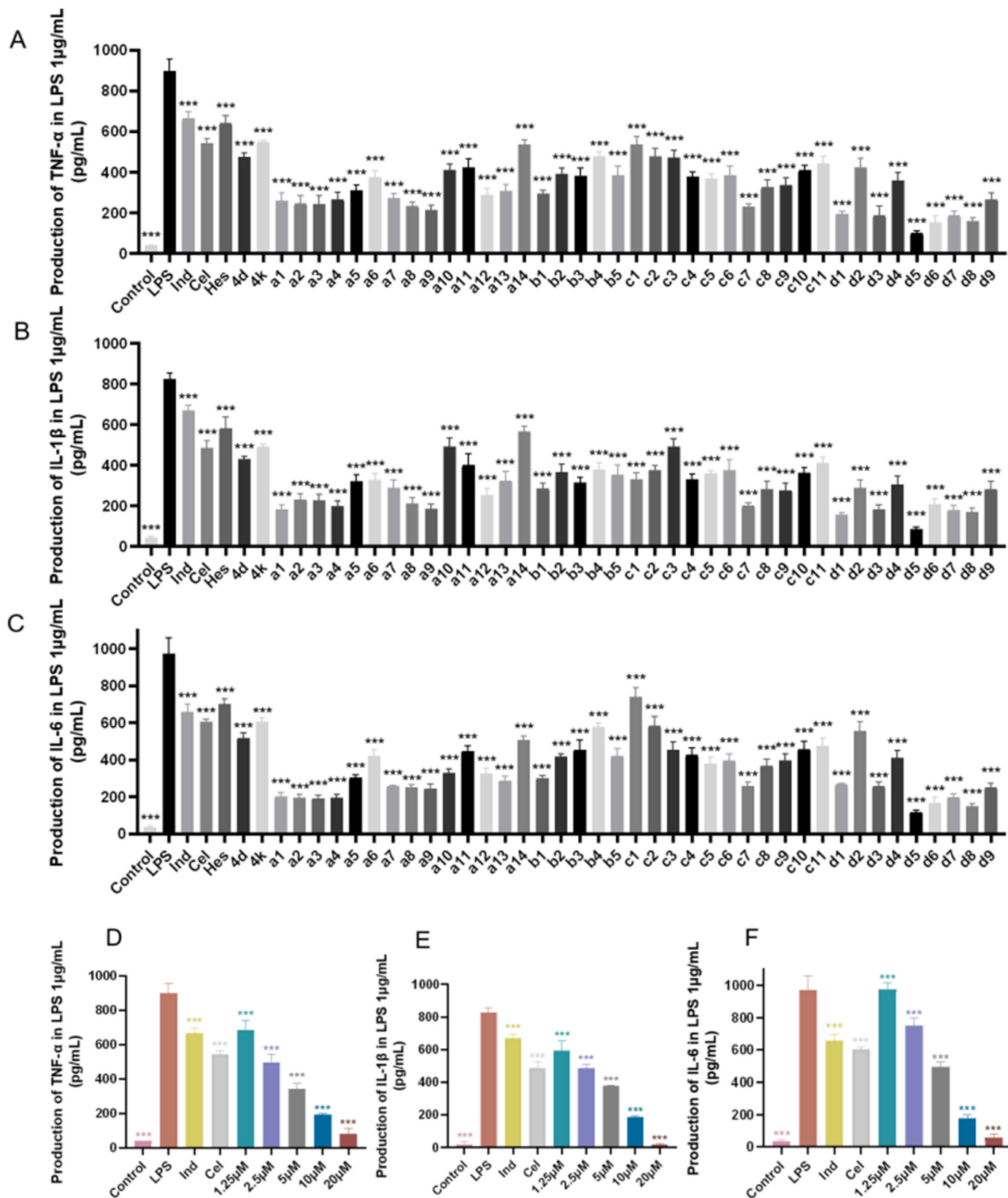


**Fig. 3.** ELISA kit was used to evaluate the inflammatory factor inhibiting the action of compounds on RAW 264.7 cells under LPS stimulation. All compounds were tested to release TNF- $\alpha$ , IL-1 $\beta$ , and IL-6 from LPS-stimulated RAW264.7 cells at a concentration of 10  $\mu$ M (A–C). Compound **d5** showed the best suppression effect in the primary screening. We tested the inhibitory effect of **d5** on LPS-induced inflammatory factors in RAW264.7 cells at different concentrations (D–F). The difference was considered statistically significant when p (\*) < 0.05, (\*\*) < 0.01, (\*\*\*) < 0.001 vs LPS group. Hes: hesperetin, Ind: indomethacin, Cel: celecoxib vs. LPS group.

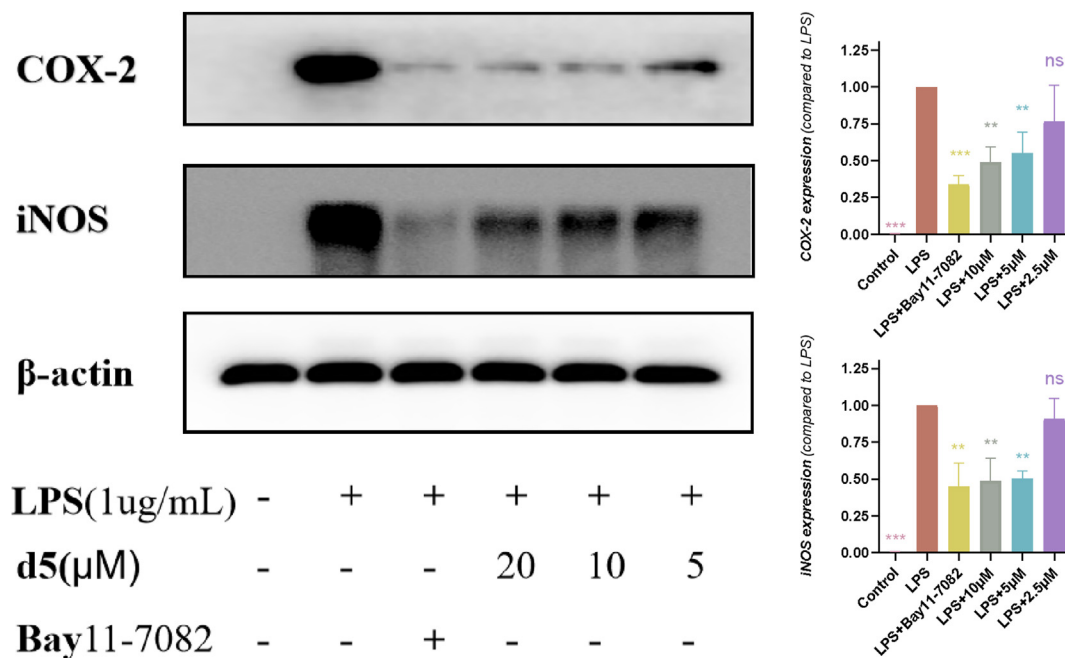


**Fig. 4.** Compound **d5** suppressed the expression levels of COX-2 and iNOS in RAW264.7 cells stimulated by LPS. The difference was considered statistically significant when  $p$  (\*) < 0.05, (\*\*) < 0.01, (\*\*\*) < 0.001. ns: no significance vs LPS group.

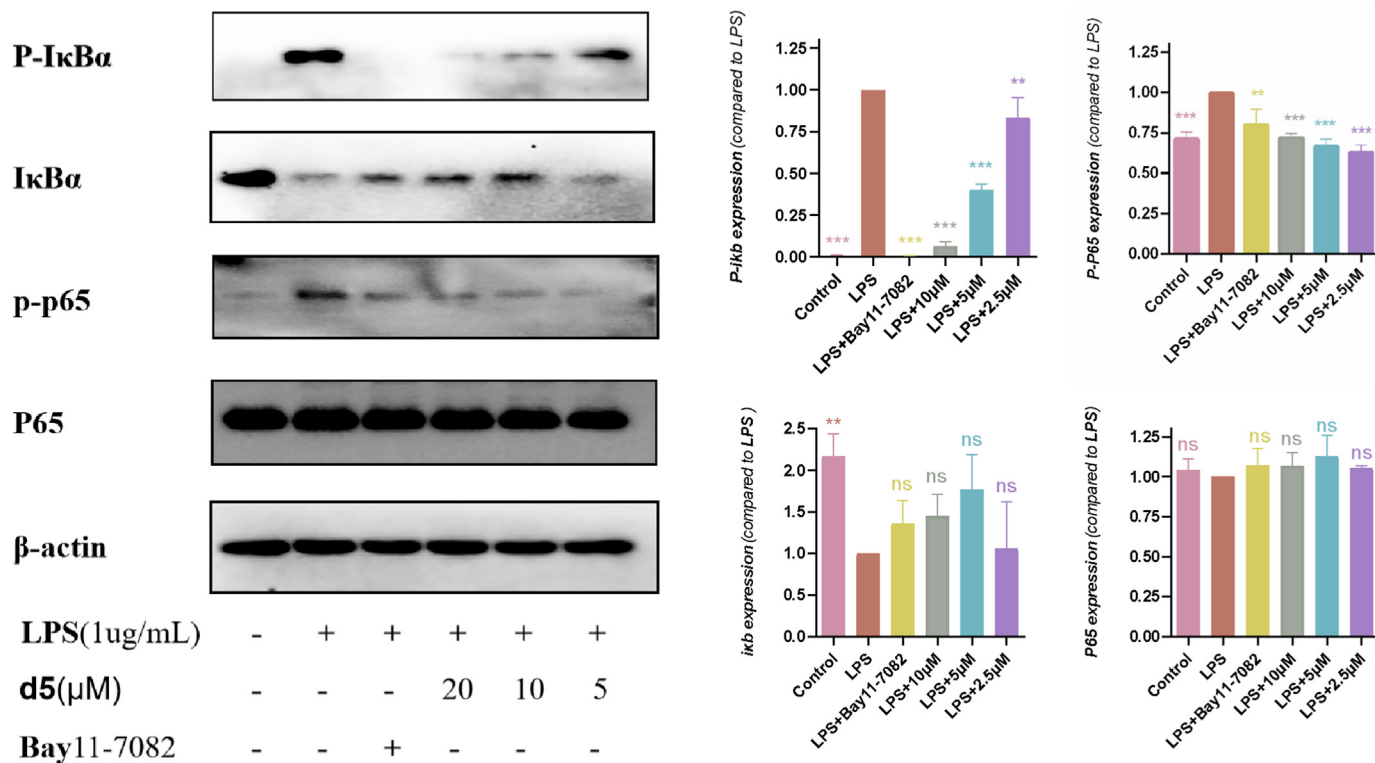


**Fig. 5.** Compound **d5** regulates the inflammatory effect of RAW264.7 cells by LPS stimulation through negatively regulating the NF-κB signaling pathway. The difference was considered statistically significant when  $p$  (\*) < 0.05, (\*\*) < 0.01, (\*\*\*) < 0.001. ns: no significance.

2.2.6. Inhibition of ROS production

ROS, including superoxide radicals, hydrogen peroxide, and its downstream products, peroxides, and hydroxides, are involved in the occurrence and development of many kinds of inflammation [46,47]. ROS detection kit is a technique that uses fluorescent probe

2'-7'dichlorofluorescein diacetate (DCFH-DA) to detect ROS. DCFH-DA can freely pass through the cell membrane, enter the cell, and hydrolyze to form DCFH, which cannot cross the cell membrane, thus limiting the cell. The green fluorescence intensities of DCF and DCFH oxidation to produce fluorescent substances are proportional

to intracellular ROS levels, indirectly reflecting the level of ROS in the cell. The inhibitory effects of compound **d5** (10, 5, and 2.5  $\mu\text{M}$ ) under different concentrations during ROS production stimulation were detected by flow cytometry. The results are shown in Fig. 6. The values of ROS expression in the LPS stimulation group were significantly higher than that in the control group. This finding suggests that the models were established successfully. After treatment with derivative **d5**, the expression of ROS was lower than that of the stimulation group, and the ROS content of RAW264.7 cells stimulated by LPS decreased accordingly. Thus, compound **d5** can reduce the ROS production of LPS-stimulated RAW264.7 cells in a concentration-dependent manner. Furthermore, the anti-inflammatory effects of compound **d5** partly inhibited the production of ROS in the inflammatory state.

### 2.3. In vivo pharmacology

#### 2.3.1. Compound **d5** can alleviate histopathological changes in a mouse model of ALI induced by $\text{CCl}_4$

ALI caused by intraperitoneal injection of  $\text{CCl}_4$  in mice is one of the most commonly used inflammation models [48,49].  $\text{CCl}_4$  can be rapidly absorbed after entering hepatocytes and activated by binding to cytochrome  $\text{P}_{450}$  of hepatocytes to produce harmful free radicals and destroy the structure and function of biofilms, thereby destroying the structure of liver cell biofilms, which ultimately leads to liver apoptosis and necrosis.

As shown in Fig. 7A, the livers of normal control mice were ruddy, and the livers surfaces were smooth. However, the livers of mice with liver injury induced by  $\text{CCl}_4$  turned pale yellow, and necrosis of yellow spots was visible to the naked eyes. Fig. 7B shows the hematoxylin and eosin (HE)-stained liver tissue; the normal group's liver cells were regularly arranged, the liver sinus structures were clear, and liver lobules were intact.  $\text{CCl}_4$ -induced ALI in mice showed evident hepatocyte necrosis, vacuoles, irregular arrangement of hepatic cords, unclear or disappearing cell boundaries, and inflammatory cell infiltration, but no such lesions were recorded in the normal group. The liver tissue damage was alleviated in mice treated with different concentrations of compound **d5** (50, 100, and 200 mg/kg) and silymarin (200 mg/kg). The mice given with compound **d5** in the high-dose group showed comparable anti-inflammatory and liver protection effects with the positive control drugs.

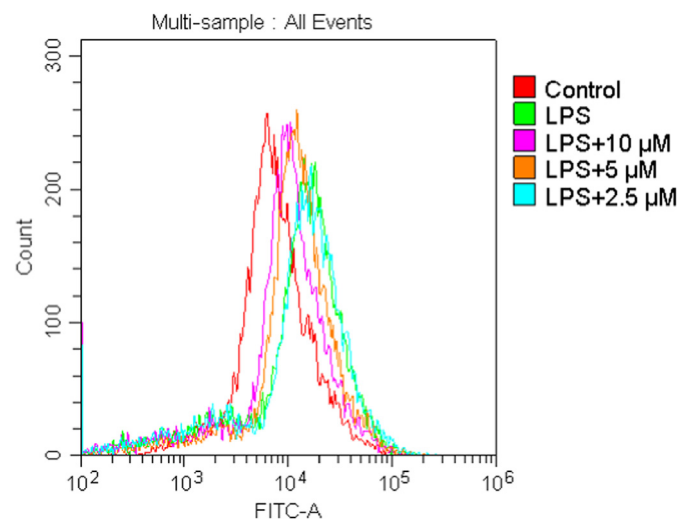


Fig. 6. ROS of RAW264.7 cells were determined by the fluorescent probe DCFH-DA on compound **d5** compared with the LPS group.

#### 2.3.2. Compound **d5** can alleviate the increase in liver markers and cytokine production in the $\text{CCl}_4$ -induced ALI mouse model

$\text{CCl}_4$  induces ALI, destroys the cell biofilm structure, causes transaminases in the liver cells to overflow, and increases the content of alanine aminotransferase (ALT) and aspartate aminotransferase (AST) in the blood. The increase in biochemical indicators of liver enzymes occurs due to the destruction of liver cell structural integrity [50]. Serum levels of ALT and AST were determined using ALT and AST activity assay kits. As shown in Fig. 8A and B, the levels of ALT and AST in mice in the normal group were below 40 U/L, whereas those in the model group had greatly increased. The low-, medium-, and high-dose compound **d5** and silymarin can reduce serum ALT and AST levels, with **d5** in the high-dose group showing higher effectivity in reducing ALT and AST than the silymarin control group.

ALI induced by  $\text{CCl}_4$  stimulates macrophages to release inflammatory cytokines, further aggravating liver damage [51]. Thus, we used ELISA to detect serum inflammatory factors  $\text{TNF-}\alpha$ ,  $\text{IL-1}\beta$ , and  $\text{IL-6}$  levels. As shown in Fig. 8C–E, in normal state, the levels of inflammatory factors in serum were low. Cytokines  $\text{TNF-}\alpha$ ,  $\text{IL-1}\beta$ , and  $\text{IL-6}$  in the model group had greatly increased. The content of inflammatory factors in **d5** and silymarin groups was lower than those in the model group. The above results indicate that compound **d5** exerts hepatoprotective effect on ALI in mice and an inhibitory effects on the inflammatory response during ALI.

## 3. Materials and methods

### 3.1. Chemistry

#### 3.1.1. General

The reagents needed in the experiment are purchased through formal commercial channels. SGW®X-4A melting point detector was used to measure the melting point of the compound (Shanghai Instrument Physical Optical Instrument Co., Ltd., Shanghai, China). The  $^1\text{H}$  NMR and  $^{13}\text{C}$  NMR spectra of the compound were detected in dimethyl sulfoxide ( $\text{DMSO-}d_6$ ) using a Bruker AV-400MHz instrument. The tetramethylsilane (TMS) signal drop in parts per million ( $\delta$ ) is used as the internal standard to indicate the chemical shift. Hz is the unit of coupling constant. Use s (single peak), d (double peak), t (triplet), br (wide), or m (multimodal) to define multiplicity. Use Agilent 1260–6221 TOF mass spectrometer to analyze and obtain high-resolution mass spectra. Column chromatography (CC) uses silica gel (200–300 mesh) to separate. Thin-layer chromatography (TLC) uses silica gel GF254 (Qingdao Ocean Chemical Factory) for analysis.

#### 3.1.2. Synthetic methods of all compounds

3.1.2.1. *Synthesis of hesperetin (1)*. Hesperidin (72 g, 0.12 mol) was added to the pre-configured ethanol (640 mL) and 98%  $\text{H}_2\text{SO}_4$  (80 mL) mixed solution, and the suspension was heated to reflux (80  $^\circ\text{C}$ , 8 h). The reaction solution was cooled to room temperature and put into 2 L volume of ice water. The precipitate was collected by filtration, washed with water and dried. The mixture was dissolved by ethanol and heated to reflux for 1 h. After cooled, added activated carbon to the solution for 15 min. The solution was filtered and washed with hot ethanol. The ethanol solution was concentrated under reduced pressure, and the residue was recrystallized from ethanol and  $\text{CH}_2\text{Cl}_2$  to obtain hesperetin (**1**) (white powder, 31.5 g, yield 87%), m.p. 229.5–231.6  $^\circ\text{C}$ ;  $^1\text{H}$  NMR (400 MHz,  $\text{DMSO}$ )  $\delta$  12.14 (s, 1H, 5-OH), 10.80 (s, 1H, 7-OH), 9.11 (s, 1H, 3'-OH), 6.95–6.92 (m,  $J = 5.1, 3.2$  Hz, 2H, 2'-H, 5'-H), 6.87 (dd,  $J = 8.3, 2.0$  Hz, 1H, 6'-H), 5.89 (d,  $J = 2.1$  Hz, 1H, 8-H), 5.88 (d,  $J = 2.1$  Hz, 1H, 6-H), 5.43 (dd,  $J = 12.4, 3.0$  Hz, 1H, 2-H), 3.77 (s, 3H,  $\text{OCH}_3$ ), 3.20 (dd,  $J = 17.1, 12.4$  Hz, 1H, 3-H), 2.70 (dd,  $J = 17.1, 3.1$  Hz,

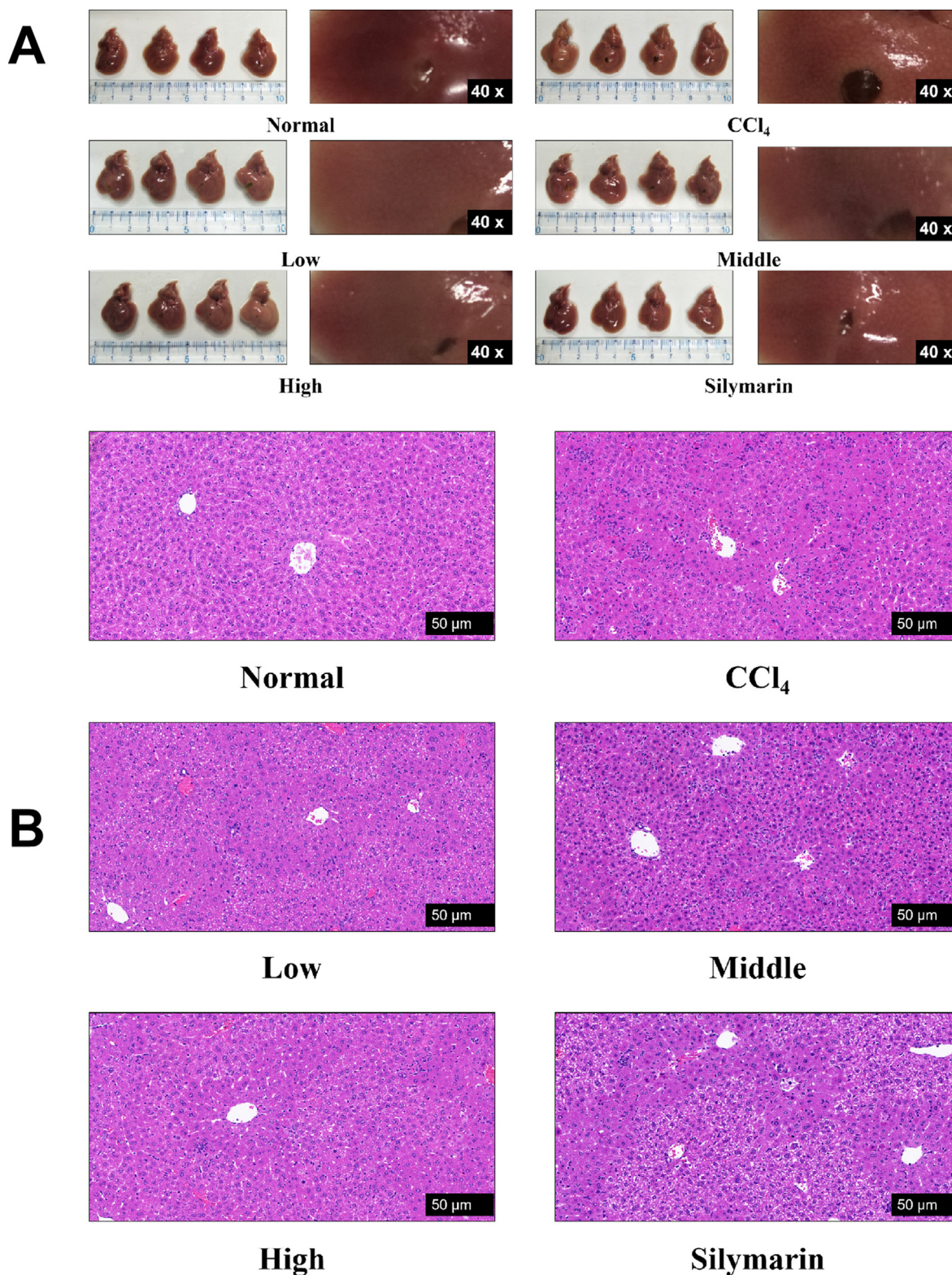


**Fig. 7.** Pathological manifestation of the protective effect of compound **d5** on the liver of model mice. (A) Representative images of fresh livers from different groups. (B) Pathological microscopic ( $\times 20$ ) observation of mouse liver tissue sections stained with HE. Compound **d5** in the low- (50 mg/kg), middle- (100 mg/kg), and high-dose group (200 mg/kg) and silymarin group (200 mg/kg).

1H, 3-H).  $^{13}\text{C}$  NMR (101 MHz, DMSO)  $\delta$  196.61, 167.22, 163.92, 163.24, 148.34, 146.85, 131.54, 118.20, 114.45, 112.34, 102.21, 96.31, 95.49, 78.68, 56.07, 42.46. HRMS (ESI): Calcd.  $\text{C}_{16}\text{H}_{14}\text{O}_6$ ,  $[\text{M}+\text{H}]^+$   $m/z$ : 303.0875, found: 303.0881.

**3.1.2.2. Synthesis of 7-O-(prop-2-yn-1-yl)hesperetin (2).** Hesperetin (**1**) (30.2 g, 100 mmol) was added to DMF (400 mL) solution, stirred at room temperature (25 °C) for 5 min, then  $\text{K}_2\text{CO}_3$  (20.7 g, 150 mmol) was added, last propargyl bromide (23.8 g,

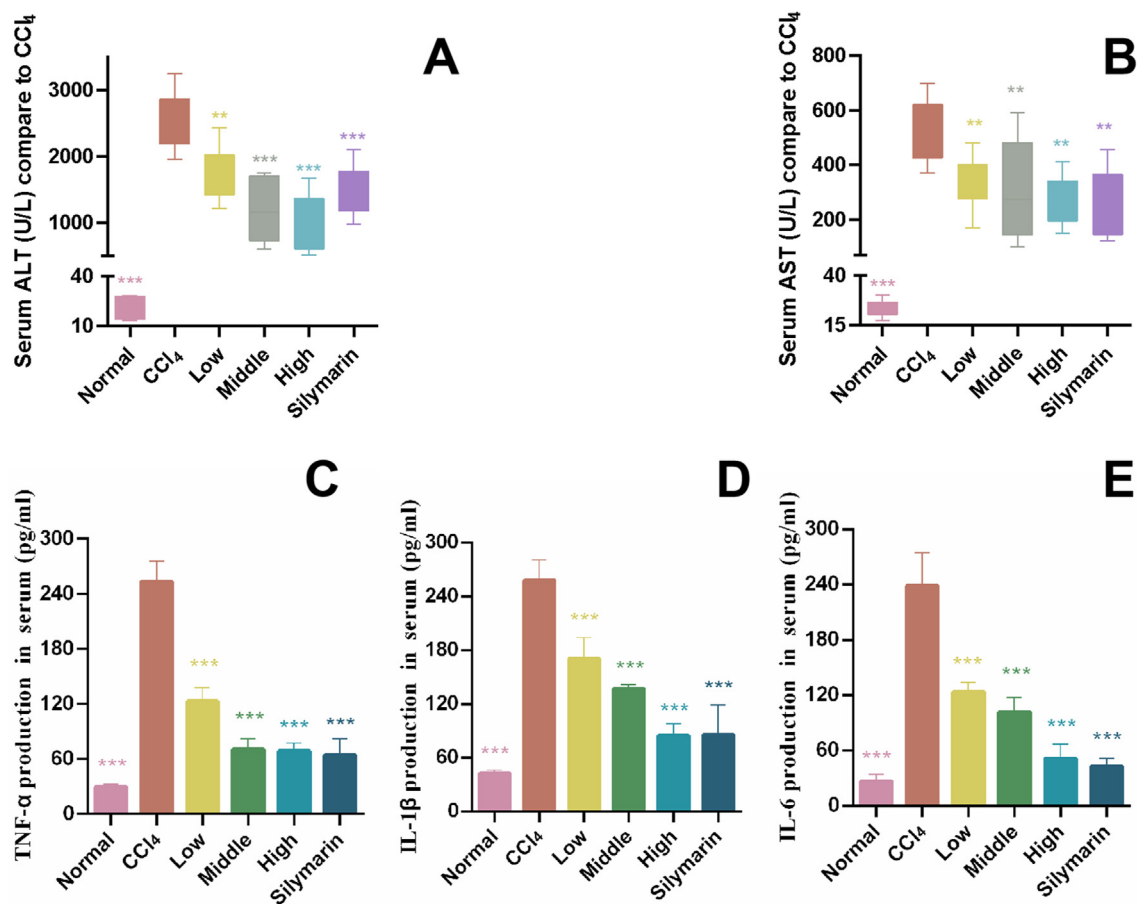


**Fig. 8.** In the CCl<sub>4</sub>-induced ALI model, compound **d5** inhibited liver markers and cytokines (A–B). Concentration-dependent alleviating effect of **d5** on ALT and AST in the ALI model (8C–8E). Concentration-dependent inhibitory effect of **d5** on TNF- $\alpha$ , IL-1 $\beta$ , and IL-6 in the ALI model. Silymarin was used as a positive control. Compound **d5** in the low- (50 mg/kg), middle- (100 mg/kg), and high-dose group (200 mg/kg); silymarin group (200 mg/kg).

200 mmol) was added. Continued to fully stir the reaction solution for 1 h, and monitored the reaction progress by thin layer chromatography. The reaction mixture was acidified with diluted HCl to pH 5–6 and extracted with EtOAc. The organic phase was washed five times with brine, dried over anhydrous Na<sub>2</sub>SO<sub>4</sub>, filtered, and concentrated under reduced pressure. The residue was recrystallized from ethanol to obtain a white crude product. The crude product was recrystallized from CH<sub>2</sub>Cl<sub>2</sub> to obtain 7-O-(prop-2-yn-1-yl)hesperetin (**2**) (white crystal powder, 16.7 g, reaction yield 49%, Scheme 1), mp: 187.3–189.8 °C; <sup>1</sup>H NMR (400 MHz, DMSO)  $\delta$  12.09 (s, 1H, 5-OH), 9.15 (s, 1H, 3'-OH), 6.94 (d,  $J$  = 8.2 Hz, 2H, 2'-H, 6-H), 6.89 (d,  $J$  = 8.2 Hz, 1H, 6'-H), 6.16 (brs, 1H, 8-H), 6.14 (brs, 1H, 6-H), 5.50 (dd,  $J$  = 12.4, 2.1 Hz, 1H, 2-H), 4.88 (s, 2H, ArOCH<sub>2</sub>), 3.78 (s, 3H, OCH<sub>3</sub>), 3.67 (s, 1H, HC $\equiv$ C), 3.29 (dd,  $J$  = 17.0, 12.8 Hz, 1H, 3-H), 2.75 (dd,  $J$  = 17.1, 2.5 Hz, 1H, 3-H). <sup>13</sup>C NMR (101 MHz, DMSO)  $\delta$  197.47, 165.63, 163.48, 163.13, 148.40, 146.92, 131.34, 118.22, 114.55, 112.34, 103.43, 95.86, 94.95, 79.47, 78.98, 78.89, 56.50, 56.08, 42.62. TOF-HRMS:  $m/z$  [M+H]<sup>+</sup>calcd for C<sub>23</sub>H<sub>20</sub>FO<sub>6</sub>: 341.1020; found: 341.1019.

**3.1.2.3. Synthesis of 4-hydroxyimino-7-O-(prop-2-yn-1-yl) hesperetin (3).** Substituent derivative (**2**, 19.4 g, 50 mmol) was dissolved by ethanol (300 mL), then hydroxylamine hydrochloride (NH<sub>2</sub>OH·HCl, 2.5 g, 36 mmol) and potassium acetate (CH<sub>3</sub>COOK, 3.5 g, 36 mmol) were added. The reaction was heated to reflux at 80 °C. The progress of the reaction was monitored using thin-layer chromatography. After 10 h, intermediate **2** was completely

reacted. The reaction solution was concentrated under reduced pressure. The resulting solid was dissolved in EtOAc (250 mL). The organic phase was extracted twice with saturated brine, dried over anhydrous Na<sub>2</sub>SO<sub>4</sub>, filtered, and concentrated under reduced pressure to obtain a white solid. The white solid was recrystallized with anhydrous ethanol to obtain the intermediate **3** as a white solid (9.4 g, yield 88%, Scheme 1), mp: 226.5–230.8 °C; <sup>1</sup>H NMR (400 MHz, DMSO)  $\delta$  11.43 (s, 1H, N–OH), 11.37 (s, 1H, 5-OH), 9.10 (s, 1H, 3'-OH), 6.93 (d,  $J$  = 7.6 Hz, 2H, 5-H, 6-H), 6.87 (d,  $J$  = 8.3 Hz, 1H, 2'-H), 6.13 (d,  $J$  = 1.3 Hz, 2H, 6-H, 8-H), 5.10 (dd,  $J$  = 11.4, 2.8 Hz, 1H, 2-H), 4.78 (d,  $J$  = 1.9 Hz, 2H, OCH<sub>2</sub>C $\equiv$ C), 3.78 (s, 3H, OCH<sub>3</sub>), 3.60 (s, 1H, C $\equiv$ CH), 3.30 (dd,  $J$  = 17.0, 3.0 Hz, 1H, 3-H), 2.80 (dd,  $J$  = 17.1, 11.5 Hz, 1H, 3-H). <sup>13</sup>C NMR (101 MHz, DMSO)  $\delta$  160.12, 159.33, 158.08, 153.33, 148.14, 146.89, 132.38, 117.89, 114.33, 112.37, 99.23, 96.37, 95.06, 79.46, 78.94, 76.25, 56.06, 55.99, 29.42. TOF-HRMS:  $m/z$  [M+H]<sup>+</sup>calcd for C<sub>23</sub>H<sub>20</sub>FO<sub>6</sub>: 356.1129; found: 356.1132.

### 3.1.3. General procedure for the synthesis of **a1-a14**, **c1-c11**

To a solution of bromide (2.2 mmol) in DMF (50 mL) Na<sub>3</sub> (143 mg, 2.2 mmol) was added. After stirred at r.t for 3 h, the solid disappeared completely. Added ascorbic acid (528 mg, 3 mmol) and anhydrous K<sub>2</sub>CO<sub>3</sub> (414 mg, 3 mmol) into the reaction solution, stirred at r.t for 30 min. Then added the intermediate **2** (680 mg, 2 mmol) and CuSO<sub>4</sub>·5H<sub>2</sub>O (625 mg, 2.5 mmol) into the reaction solution, stirred at r.t for 3 h. The method as described in 4.1.2.2 (acidified to pH 5–6 and extracted with EtOAc, washed with brine solution, dried over anhydrous Na<sub>2</sub>SO<sub>4</sub>, filtered, and concentrated).

The residue was recrystallized from ethanol and  $\text{CH}_2\text{Cl}_2$  to obtain triazoles **a1**–**a14** and **c1**–**c9**. The residues of **c10**, **c11** were purified by flash column chromatography ( $\text{CHCl}_3$ /Petroleum ether/mehanol = 50/50/1, v/v/v) [30] (white crystal or powder, yield 36–80% for this step reaction, Scheme 1).

**3.1.3.1. 7-O-((1-(2-benzyl-1H-1,2,3-triazol-4-yl)methyl)hesperetin (a1).** White crystal, 83% yield, m.p. 221.2–223.8 °C;  $^1\text{H}$  NMR (400 MHz, DMSO)  $\delta$  12.15 (s, 1H, 5-OH), 9.18 (s, 1H, 3'-OH), 8.36 (s, 1H, NC=CHN), 7.45–7.34 (m, 5H, ArH), 7.01–6.96 (m, 2H, 2'-H, 5'-H), 6.93 (dd,  $J$  = 8.4, 1.9 Hz, 1H, 6'-H), 6.26 (d,  $J$  = 2.2 Hz, 1H, 8-H), 6.24 (d,  $J$  = 2.2 Hz, 1H, 6-H), 5.66 (s, 2H,  $\text{ArCH}_2\text{N}$ ), 5.53 (dd,  $J$  = 12.5, 2.9 Hz, 1H, 2-H), 5.24 (s, 2H,  $\text{ArOCH}_2$ ), 3.82 (s, 3H,  $\text{OCH}_3$ ), 3.31 (dd,  $J$  = 17.2, 12.5 Hz, 1H, 3-H), 2.79 (dd,  $J$  = 17.1, 3.0 Hz, 1H, 3-H).  $^{13}\text{C}$  NMR (101 MHz, DMSO)  $\delta$  197.35, 166.55, 163.60, 163.20, 148.41, 146.93, 142.59, 136.42, 131.39, 129.26, 129.26, 128.67, 128.48, 128.48, 125.49, 118.23, 114.58, 112.39, 103.26, 95.77, 94.88, 78.94, 62.06, 56.11, 53.33, 42.60. TOF-HRMS:  $m/z$   $[\text{M}+\text{H}]^+$  calcd for  $\text{C}_{24}\text{H}_{23}\text{O}_6$ : 474.1660; found: 474.1658.

**3.1.3.2. 7-O-((1-(2-methylbenzyl)-1H-1,2,3-triazol-4-yl)methyl)hesperetin (a2).** White crystal, 85% yield, m.p. 222.6–225.2 °C;  $^1\text{H}$  NMR (400 MHz, DMSO)  $\delta$  12.10 (s, 1H, 5-OH), 9.15 (s, 1H, 3'-OH), 8.22 (s, 1H, NC=CHN), 7.29–7.16 (m, 3H, ArH), 7.10 (d,  $J$  = 7.4 Hz, 1H, ArH), 6.98–6.92 (m, 2H, 2'-H, 5'-H), 6.90 (d,  $J$  = 8.2 Hz, 1H, 6'-H), 6.22 (brs, 1H, 8-H), 6.20 (brs, 1H, 6-H), 5.64 (s, 2H,  $\text{ArCH}_2\text{N}$ ), 5.49 (dd,  $J$  = 12.3, 2.5 Hz, 1H, 2-H), 5.21 (s, 2H,  $\text{ArOCH}_2$ ), 3.78 (s, 3H,  $\text{OCH}_3$ ), 3.28 (dd,  $J$  = 17.1, 12.6 Hz, 1H, 3-H), 2.76 (dd,  $J$  = 17.1, 2.7 Hz, 1H, 3-H), 2.32 (s, 3H,  $\text{ArCH}_3$ ).  $^{13}\text{C}$  NMR (101 MHz, DMSO)  $\delta$  197.35, 166.54, 163.59, 163.19, 148.41, 146.93, 142.47, 136.81, 134.52, 131.39, 130.93, 129.19, 128.85, 126.75, 125.56, 118.24, 114.58, 112.38, 103.25, 95.79, 94.90, 78.94, 62.03, 56.10, 51.45, 42.60, 19.11; TOF-HRMS:  $m/z$   $[\text{M}+\text{H}]^+$  calcd for  $\text{C}_{24}\text{H}_{23}\text{O}_6$ : 488.1816; found: 488.1816.

**3.1.3.3. 7-O-((1-(2-fluorobenzyl)-1H-1,2,3-triazol-4-yl)methyl)hesperetin (a3).** White crystal, 81% yield, m.p. 231.4–234.6 °C;  $^1\text{H}$  NMR (400 MHz, DMSO)  $\delta$  12.11 (s, 1H, 5-OH), 9.14 (s, 1H, 3'-OH), 8.31 (s, 1H, NC=CHN), 7.47–7.34 (m, 2H, ArH), 7.30–7.20 (m, 2H, ArH), 6.95 (dd,  $J$  = 5.0, 3.1 Hz, 2H, 2'-H, 5'-H), 6.90 (dd,  $J$  = 8.3, 1.8 Hz, 1H, 6'-H), 6.23 (d,  $J$  = 2.2 Hz, 1H, 8-H), 6.20 (d,  $J$  = 2.2 Hz, 1H, 6-H), 5.69 (s, 2H,  $\text{ArCH}_2\text{N}$ ), 5.49 (dd,  $J$  = 12.4, 2.9 Hz, 1H, 2-H), 5.21 (s, 2H,  $\text{ArOCH}_2$ ), 3.78 (s, 3H,  $\text{OCH}_3$ ), 3.28 (dd,  $J$  = 17.2, 12.5 Hz, 1H, 3-H), 2.76 (dd,  $J$  = 17.1, 3.0 Hz, 1H, 3-H).  $^{13}\text{C}$  NMR (101 MHz, DMSO)  $\delta$  197.35, 166.54, 163.59, 163.20, 160.58 ( $^1J$  = 246.6 Hz), 148.41, 146.93, 142.50, 131.39, 131.31 ( $^2J$  = 3.5 Hz), 131.26, 125.67, 125.34 ( $^2J$  = 3.5 Hz), 123.22 ( $^2J$  = 14.7 Hz), 118.23, 116.13 ( $^2J$  = 20.9 Hz), 114.58, 112.39, 103.26, 95.76, 94.88, 78.94, 61.99, 56.11, 47.42 ( $^3J$  = 3.8 Hz), 42.60; TOF-HRMS:  $m/z$   $[\text{M}+\text{H}]^+$  calcd for  $\text{C}_{24}\text{H}_{23}\text{O}_6$ : 492.1565; found: 492.1565.

**3.1.3.4. 7-O-((1-(2-chlorobenzyl)-1H-1,2,3-triazol-4-yl)methyl)hesperetin (a4).** White crystal, 78% yield, m.p. 234.1–236.9 °C;  $^1\text{H}$  NMR (400 MHz, DMSO)  $\delta$  12.11 (s, 1H, 5-OH), 9.14 (s, 1H, 3'-OH), 8.30 (s, 1H, NC=CHN), 7.53 (dd,  $J$  = 7.6, 1.6 Hz, 1H, ArH), 7.44–7.35 (m, 2H, ArH), 7.26 (dd,  $J$  = 7.3, 1.9 Hz, 1H, ArH), 6.97–6.92 (m, 2H, 2'-H, 5'-H), 6.90 (dd,  $J$  = 8.3, 1.9 Hz, 1H, 6'-H), 6.23 (d,  $J$  = 2.2 Hz, 1H, 8-H), 6.20 (d,  $J$  = 2.2 Hz, 1H, 6-H), 5.74 (s, 2H,  $\text{ArCH}_2\text{N}$ ), 5.49 (dd,  $J$  = 12.5, 2.9 Hz, 1H, 2-H), 5.22 (s, 2H,  $\text{ArOCH}_2$ ), 3.78 (s, 3H,  $\text{OCH}_3$ ), 3.28 (dd,  $J$  = 17.2, 12.5 Hz, 1H, 3-H), 2.76 (dd,  $J$  = 17.2, 3.1 Hz, 1H, 3-H).  $^{13}\text{C}$  NMR (101 MHz, DMSO)  $\delta$  197.35, 166.53, 163.59, 163.20, 148.41, 146.93, 142.43, 133.64, 133.14, 131.39, 131.05, 130.78, 130.13, 128.22, 125.92, 118.23, 114.58, 112.38, 103.26, 95.79, 94.90, 78.94, 61.99, 56.11, 51.13, 42.61; TOF-HRMS:  $m/z$   $[\text{M}+\text{H}]^+$  calcd for  $\text{C}_{24}\text{H}_{20}\text{NO}_6$ : 508.1270; found: 508.1266.

**3.1.3.5. 7-O-((1-(2-cyanobenzyl)-1H-1,2,3-triazol-4-yl)methyl)hesperetin (a5).** White powder, 77% yield, m.p. 240.8–245.0 °C;  $^1\text{H}$  NMR (400 MHz, DMSO)  $\delta$  12.11 (s, 1H, 5-OH), 9.16 (s, 1H, 3'-OH), 8.38 (s, 1H, NC=CHN), 7.93 (d,  $J$  = 7.6 Hz, 1H, ArH), 7.73 (t,  $J$  = 7.6 Hz, 1H, ArH), 7.57 (t,  $J$  = 7.5 Hz, 1H, ArH), 7.39 (d,  $J$  = 7.7 Hz, 1H, ArH), 6.94 (d,  $J$  = 7.8 Hz, 2H, 2'-H, 5'-H), 6.90 (d,  $J$  = 8.2 Hz, 1H, 6'-H), 6.23 (brs, 1H, 8-H), 6.21 (brs, 1H, 6-H), 5.85 (s, 2H,  $\text{ArCH}_2\text{N}$ ), 5.49 (d,  $J$  = 11.9 Hz, 1H, 2-H), 5.23 (s, 2H,  $\text{ArOCH}_2$ ), 3.78 (s, 3H,  $\text{OCH}_3$ ), 3.28 (dd,  $J$  = 16.9, 12.7 Hz, 1H, 3-H), 2.75 (d,  $J$  = 16.8 Hz, 1H, 3-H).  $^{13}\text{C}$  NMR (101 MHz, DMSO)  $\delta$  197.37, 166.51, 163.60, 163.20, 148.40, 146.91, 142.61, 139.16, 134.33, 133.87, 131.37, 129.93, 129.73, 126.01, 118.24, 117.48, 114.58, 112.35, 111.73, 103.27, 95.78, 94.89, 78.95, 61.97, 56.08, 51.53, 42.60; TOF-HRMS:  $m/z$   $[\text{M}+\text{H}]^+$  calcd for  $\text{C}_{24}\text{H}_{20}\text{NO}_6$ : 499.1612; found: 499.1614.

**3.1.3.6. 7-O-((1-(2-(trifluoromethyl)benzyl)-1H-1,2,3-triazol-4-yl)methyl)hesperetin (a6).** White crystal, 80% yield, m.p. 242.1–245.5 °C;  $^1\text{H}$  NMR (400 MHz, DMSO)  $\delta$  12.12 (s, 1H, 5-OH), 9.15 (s, 1H, 3'-OH), 8.32 (s, 1H, NC=CHN), 7.82 (d,  $J$  = 7.8 Hz, 1H, ArH), 7.69 (t,  $J$  = 7.6 Hz, 1H, ArH), 7.59 (t,  $J$  = 7.6 Hz, 1H, ArH), 7.20 (d,  $J$  = 7.7 Hz, 1H, ArH), 6.95 (d,  $J$  = 8.0 Hz, 2H, 2'-H, 5'-H), 6.90 (d,  $J$  = 8.3 Hz, 1H, 6'-H), 6.23 (brs, 1H, 8-H), 6.21 (brs, 1H, 6-H), 5.83 (s, 2H,  $\text{ArCH}_2\text{N}$ ), 5.49 (dd,  $J$  = 12.4, 2.5 Hz, 1H, 2-H), 5.23 (s, 2H,  $\text{ArOCH}_2$ ), 3.78 (s, 3H,  $\text{OCH}_3$ ), 3.28 (dd,  $J$  = 17.1, 12.6 Hz, 1H, 3-H), 2.76 (dd,  $J$  = 17.1, 2.7 Hz, 1H, 3-H).  $^{13}\text{C}$  NMR (101 MHz, DMSO)  $\delta$  197.36, 166.52, 163.60, 163.20, 148.40, 146.92, 142.57, 134.04 ( $^3J$  = 1.4 Hz), 133.65, 131.37, 130.80, 129.42, 127.07 ( $^2J$  = 30.1 Hz), 126.70 ( $^3J$  = 5.0 Hz), 126.17, 124.59 ( $^1J$  = 273.9 Hz), 118.23, 114.58, 112.35, 103.26, 95.79, 94.90, 78.95, 61.98, 56.08, 50.07 ( $^4J$  = 2.2 Hz), 42.60; TOF-HRMS:  $m/z$   $[\text{M}+\text{H}]^+$  calcd for  $\text{C}_{24}\text{H}_{20}\text{NO}_6$ : 542.1533; found: 542.1535.

**3.1.3.7. 7-O-((1-(3-methylbenzyl)-1H-1,2,3-triazol-4-yl)methyl)hesperetin (a7).** White crystal, 81% yield, m.p. 233.8–236.3 °C;  $^1\text{H}$  NMR (400 MHz, DMSO)  $\delta$  12.11 (s, 1H, 5-OH), 9.14 (s, 1H, 3'-OH), 8.31 (s, 1H, NC=CHN), 7.30–7.23 (m, 1H, ArH), 7.14 (dd,  $J$  = 11.1, 5.0 Hz, 3H, ArH), 6.97–6.92 (m, 2H, 2'-H, 5'-H), 6.89 (dd,  $J$  = 8.3, 1.9 Hz, 1H, 6'-H), 6.23 (d,  $J$  = 2.2 Hz, 1H, 8-H), 6.20 (d,  $J$  = 2.2 Hz, 1H, 6-H), 5.57 (s, 2H,  $\text{ArCH}_2\text{N}$ ), 5.49 (dd,  $J$  = 12.5, 2.9 Hz, 1H, 2-H), 5.20 (s, 2H,  $\text{ArOCH}_2$ ), 3.78 (s, 3H,  $\text{OCH}_3$ ), 3.27 (dd,  $J$  = 17.2, 12.5 Hz, 1H, 3-H), 2.75 (dd,  $J$  = 17.1, 3.0 Hz, 1H, 3-H), 2.29 (s, 3H,  $\text{ArCH}_3$ ).  $^{13}\text{C}$  NMR (101 MHz, DMSO)  $\delta$  197.35, 166.54, 163.60, 163.19, 148.41, 146.93, 142.56, 138.50, 136.30, 131.39, 129.30, 129.17, 129.06, 125.61, 125.45, 118.23, 114.58, 112.39, 103.26, 95.76, 94.89, 78.94, 62.06, 56.11, 53.34, 42.60, 21.38; TOF-HRMS:  $m/z$   $[\text{M}+\text{H}]^+$  calcd for  $\text{C}_{24}\text{H}_{20}\text{F}_3\text{O}_6$ : 488.1816; found: 488.1813.

**3.1.3.8. 7-O-((1-(3-chlorobenzyl)-1H-1,2,3-triazol-4-yl)methyl)hesperetin (a8).** White powder, 79% yield, m.p. 245.2–249.1 °C;  $^1\text{H}$  NMR (400 MHz, DMSO)  $\delta$  12.11 (s, 1H, 5-OH), 9.14 (s, 1H, 3'-OH), 8.36 (s, 1H, NC=CHN), 7.45–7.38 (m, 3H, ArH), 7.32–7.26 (m, 1H, ArH), 6.95 (dd,  $J$  = 5.0, 3.1 Hz, 2H, 2'-H, 5'-H), 6.89 (dd,  $J$  = 8.4, 1.8 Hz, 1H, 6'-H), 6.23 (d,  $J$  = 2.2 Hz, 1H, 8-H), 6.20 (d,  $J$  = 2.2 Hz, 1H, 6-H), 5.65 (s, 2H,  $\text{ArCH}_2\text{N}$ ), 5.49 (dd,  $J$  = 12.5, 2.9 Hz, 1H, 2-H), 5.22 (s, 2H,  $\text{ArOCH}_2$ ), 3.78 (s, 3H,  $\text{OCH}_3$ ), 3.28 (dd,  $J$  = 17.1, 12.5 Hz, 1H, 3-H), 2.76 (dd,  $J$  = 17.1, 3.0 Hz, 1H, 3-H).  $^{13}\text{C}$  NMR (101 MHz, DMSO)  $\delta$  197.35, 166.52, 163.60, 163.20, 148.41, 146.93, 142.68, 138.78, 133.77, 131.39, 131.21, 128.67, 128.40, 127.22, 125.65, 118.23, 114.58, 112.39, 103.27, 95.77, 94.88, 78.94, 62.03, 56.11, 52.55, 42.60; TOF-HRMS:  $m/z$   $[\text{M}+\text{H}]^+$  calcd for  $\text{C}_{24}\text{H}_{20}\text{F}_3\text{O}_6$ : 508.1270; found: 508.1274.

**3.1.3.9. 7-O-((1-(3-cyanobenzyl)-1H-1,2,3-triazol-4-yl)methyl)hesperetin (a9).** White powder, 71% yield, m.p. 250.8–255.1 °C;  $^1\text{H}$  NMR (400 MHz, DMSO)  $\delta$  12.15 (s, 1H, 5-OH), 9.18 (s, 1H, 3'-OH),

8.42 (s, 1H, NC=CHN), 7.88 (d,  $J = 8.6$  Hz, 2H, ArH), 7.70 (d,  $J = 7.9$  Hz, 1H, ArH), 7.64 (t,  $J = 7.7$  Hz, 1H, ArH), 7.02–6.96 (m, 2H, 2'-H, 5'-H), 6.93 (dd,  $J = 8.4, 1.8$  Hz, 1H, 6'-H), 6.27 (d,  $J = 2.2$  Hz, 1H, 8-H), 6.24 (d,  $J = 2.2$  Hz, 1H, 6-H), 5.75 (s, 2H, ArCH<sub>2</sub>N), 5.53 (dd,  $J = 12.4, 2.9$  Hz, 1H, 2-H), 5.26 (s, 2H, ArOCH<sub>2</sub>), 3.82 (s, 3H, OCH<sub>3</sub>), 3.32 (dd,  $J = 17.1, 12.5$  Hz, 1H, 3-H), 2.80 (dd,  $J = 17.1, 3.0$  Hz, 1H, 3-H). <sup>13</sup>C NMR (101 MHz, DMSO)  $\delta$  197.35, 166.51, 163.60, 163.20, 148.41, 146.92, 142.74, 137.91, 133.50, 132.53, 132.24, 131.38, 130.59, 125.72, 118.90, 118.24, 114.59, 112.38, 112.18, 103.27, 95.76, 94.88, 78.95, 62.03, 56.10, 52.38, 42.60; TOF-HRMS:  $m/z$  [M+H]<sup>+</sup>calcd for C<sub>24</sub>H<sub>20</sub>F<sub>3</sub>O<sub>6</sub>: 499.1612; found: 499.1608.

**3.1.3.10.** 7-O-((1-(3-(trifluoromethyl)benzyl)-1H-1,2,3-triazol-4-yl)methyl)hesperetin (**a10**). White powder, 72% yield, m.p. 259.3–262.5 °C; <sup>1</sup>H NMR (400 MHz, DMSO)  $\delta$  12.15 (s, 1H, 5-OH), 9.18 (s, 1H, 3'-OH), 8.43 (s, 1H, NC=CHN), 7.82–7.73 (m, 2H, ArH), 7.68 (dd,  $J = 7.6, 5.7$  Hz, 2H, ArH), 6.99 (dd,  $J = 5.0, 3.2$  Hz, 2H, 2'-H, 5'-H), 6.93 (dd,  $J = 8.4, 1.8$  Hz, 1H, 6'-H), 6.26 (d,  $J = 2.2$  Hz, 1H, 8-H), 6.24 (d,  $J = 2.2$  Hz, 1H, 6-H), 5.79 (s, 2H, ArCH<sub>2</sub>N), 5.53 (dd,  $J = 12.5, 2.8$  Hz, 1H, 2-H), 5.26 (s, 2H, ArOCH<sub>2</sub>), 3.82 (s, 3H, OCH<sub>3</sub>), 3.32 (dd,  $J = 17.1, 12.5$  Hz, 1H, 3-H), 2.80 (dd,  $J = 17.1, 3.0$  Hz, 1H, 3-H). <sup>13</sup>C NMR (101 MHz, DMSO)  $\delta$  197.34, 166.51, 163.60, 163.20, 148.41, 146.93, 142.71, 137.79, 130.46, 129.87 (<sup>2</sup> $J = 31.8$  Hz), 125.70, 125.48 (<sup>3</sup> $J = 11.4$  Hz), 125.48 (<sup>4</sup> $J = 3.7$  Hz), 125.21 (<sup>3</sup> $J = 11.5$  Hz), 125.21 (<sup>4</sup> $J = 3.9$  Hz), 124.47 (<sup>1</sup> $J = 272.4$  Hz), 118.22, 114.58, 112.39, 103.27, 95.76, 94.88, 78.94, 62.02, 56.10, 52.59, 42.60; TOF-HRMS:  $m/z$  [M+H]<sup>+</sup>calcd for C<sub>23</sub>H<sub>21</sub>O<sub>6</sub>: 542.1533; found: 542.1529.

**3.1.3.11.** 7-O-((1-(4-methylbenzyl)-1H-1,2,3-triazol-4-yl)methyl)hesperetin (**a11**). White crystal, 75% yield, m.p. 228.4–231.0 °C; <sup>1</sup>H NMR (400 MHz, DMSO)  $\delta$  12.15 (s, 1H, 5-OH), 9.18 (s, 1H, 3'-OH), 8.31 (s, 1H, NC=CHN), 7.27 (d,  $J = 8.0$  Hz, 2H, ArH), 7.22 (d,  $J = 8.0$  Hz, 2H, ArH), 7.01–6.96 (m, 2H, 2'-H, 5'-H), 6.93 (dd,  $J = 8.3, 1.9$  Hz, 1H, 6'-H), 6.26 (d,  $J = 2.2$  Hz, 1H, 8-H), 6.23 (d,  $J = 2.2$  Hz, 1H, 6-H), 5.60 (s, 2H, ArCH<sub>2</sub>N), 5.52 (dd,  $J = 12.5, 2.9$  Hz, 1H, 2-H), 5.23 (s, 2H, ArOCH<sub>2</sub>), 3.82 (s, 3H, OCH<sub>3</sub>), 3.31 (dd,  $J = 17.1, 12.5$  Hz, 1H, 3-H), 2.79 (dd,  $J = 17.1, 3.0$  Hz, 1H, 3-H), 2.32 (s, 3H, ArCH<sub>3</sub>). <sup>13</sup>C NMR (101 MHz, DMSO)  $\delta$  197.35, 166.55, 163.59, 163.20, 148.41, 146.93, 142.54, 138.03, 133.40, 131.39, 129.78, 129.78, 128.54, 128.54, 125.33, 118.22, 114.58, 112.38, 103.26, 95.76, 94.87, 78.94, 62.05, 56.10, 53.14, 42.61, 21.16; TOF-HRMS:  $m/z$  [M+H]<sup>+</sup>calcd for C<sub>18</sub>H<sub>19</sub>O<sub>6</sub>: 488.1816; found: 488.1819.

**3.1.3.12.** 7-O-((1-(4-fluorobenzyl)-1H-1,2,3-triazol-4-yl)methyl)hesperetin (**a12**). White powder, 77% yield, m.p. 240.2–243.4 °C; <sup>1</sup>H NMR (400 MHz, DMSO)  $\delta$  12.11 (s, 1H, 5-OH), 9.14 (s, 1H, 3'-OH), 8.32 (s, 1H, NC=CHN), 7.42 (dd,  $J = 8.5, 5.6$  Hz, 2H, ArH), 7.22 (t,  $J = 8.8$  Hz, 2H, ArH), 6.97–6.93 (m, 2H, 2'-H, 5'-H), 6.89 (dd,  $J = 8.3, 1.7$  Hz, 1H, 6'-H), 6.23 (d,  $J = 2.2$  Hz, 1H, 8-H), 6.20 (d,  $J = 2.2$  Hz, 1H, 6-H), 5.62 (s, 2H, ArCH<sub>2</sub>N), 5.49 (dd,  $J = 12.4, 2.8$  Hz, 1H, 2-H), 5.20 (s, 2H, ArOCH<sub>2</sub>), 3.78 (s, 3H, OCH<sub>3</sub>), 3.28 (dd,  $J = 17.1, 12.5$  Hz, 1H, 3-H), 2.76 (dd,  $J = 17.1, 3.0$  Hz, 1H, 3-H). <sup>13</sup>C NMR (101 MHz, DMSO)  $\delta$  197.34, 166.54, 163.60, 163.20, 162.38 (<sup>1</sup> $J = 244.1$  Hz), 148.41, 146.93, 142.61, 132.66 (<sup>4</sup> $J = 3.0$  Hz), 131.39, 130.85 (<sup>3</sup> $J = 8.4$  Hz), 130.85 (<sup>2</sup> $J = 8.4$  Hz), 125.40, 118.23, 116.10 (<sup>2</sup> $J = 21.6$  Hz), 116.10 (<sup>2</sup> $J = 21.6$  Hz), 114.58, 112.39, 103.26, 95.75, 94.87, 78.94, 62.04, 56.10, 52.53, 42.60; TOF-HRMS:  $m/z$  [M+H]<sup>+</sup>calcd for C<sub>19</sub>H<sub>21</sub>O<sub>6</sub>: 492.1565; found: 492.1562.

**3.1.3.13.** 7-O-((1-(4-chlorobenzyl)-1H-1,2,3-triazol-4-yl)methyl)hesperetin (**a13**). White crystal, 70% yield, m.p. 239.1–242.2 °C; <sup>1</sup>H NMR (400 MHz, DMSO)  $\delta$  12.11 (s, 1H, 5-OH), 9.14 (s, 1H, 3'-OH), 8.33 (s, 1H, NC=CHN), 7.46 (d,  $J = 8.4$  Hz, 2H, ArH), 7.36 (d,  $J = 8.4$  Hz, 2H, ArH), 6.95 (dd,  $J = 5.1, 3.2$  Hz, 2H, 2'-H, 5'-H), 6.89 (dd,  $J = 8.4, 1.8$  Hz, 1H, 6'-H), 6.22 (d,  $J = 2.2$  Hz, 1H, 8-H), 6.20 (d,

$J = 2.2$  Hz, 1H, 6-H), 5.63 (s, 2H, ArCH<sub>2</sub>N), 5.49 (dd,  $J = 12.4, 2.9$  Hz, 1H, 2-H), 5.20 (s, 2H, ArOCH<sub>2</sub>), 3.78 (s, 3H, OCH<sub>3</sub>), 3.28 (dd,  $J = 17.1, 12.5$  Hz, 1H, 3-H), 2.76 (dd,  $J = 17.1, 3.0$  Hz, 1H, 3-H). <sup>13</sup>C NMR (101 MHz, DMSO)  $\delta$  197.35, 166.53, 163.59, 163.20, 148.41, 146.92, 142.63, 135.40, 133.40, 131.38, 130.45, 130.45, 129.26, 129.26, 125.54, 118.23, 114.58, 112.39, 103.27, 95.76, 94.88, 78.94, 62.03, 56.11, 52.51, 42.60; TOF-HRMS:  $m/z$  [M+H]<sup>+</sup>calcd for C<sub>19</sub>H<sub>19</sub>O<sub>6</sub>: 508.1270; found: 508.1262.

**3.1.3.14.** 7-O-((1-(4-(trifluoromethyl)benzyl)-1H-1,2,3-triazol-4-yl)methyl)hesperetin (**a14**). White powder, 69% yield, m.p. 246.3–250.4 °C; <sup>1</sup>H NMR (400 MHz, DMSO)  $\delta$  12.12 (s, 1H, 5-OH), 9.16 (s, 1H, 3'-OH), 8.38 (s, 1H, NC=CHN), 7.77 (d,  $J = 7.9$  Hz, 2H, ArH), 7.53 (d,  $J = 7.9$  Hz, 2H, ArH), 6.95 (d,  $J = 8.2$  Hz, 2H, 2'-H, 5'-H), 6.90 (d,  $J = 8.2$  Hz, 1H, 6'-H), 6.24 (brs, 1H, 8-H), 6.21 (brs, 1H, 6-H), 5.77 (s, 2H, ArOCH<sub>2</sub>), 5.50 (d,  $J = 12.3$  Hz, 1H, 2-H), 5.23 (s, 2H, ArOCH<sub>2</sub>), 3.78 (s, 3H, OCH<sub>3</sub>), 3.28 (dd,  $J = 17.0, 12.7$  Hz, 1H, 3-H), 2.76 (d,  $J = 17.0$  Hz, 1H, 3-H). <sup>13</sup>C NMR (101 MHz, DMSO)  $\delta$  197.36, 166.52, 163.61, 163.20, 148.40, 146.92, 142.71, 141.05, 131.37, 129.18 (<sup>2</sup> $J = 31.8$  Hz), 129.17, 129.17, 126.19 (<sup>3</sup> $J = 3.8$  Hz), 126.19 (<sup>3</sup> $J = 3.8$  Hz), 125.81, 124.55 (<sup>1</sup> $J = 272.2$  Hz), 118.22, 114.57, 112.34, 103.27, 95.76, 94.88, 78.95, 62.02, 56.07, 52.65, 42.60; TOF-HRMS:  $m/z$  [M+H]<sup>+</sup>calcd for C<sub>19</sub>H<sub>19</sub>O<sub>6</sub>: 542.1533; found: 542.1528.

**3.1.3.15.** 7-O-((1-methyl-1H-1,2,3-triazol-4-yl)methyl)hesperetin (**c1**). White crystal, 63% yield, m.p. 191.1–193.6 °C; <sup>1</sup>H NMR (400 MHz, DMSO)  $\delta$  12.11 (s, 1H, 5-OH), 9.14 (s, 1H, 3'-OH), 8.19 (s, 1H, NC=CHN), 6.94 (d,  $J = 8.4$  Hz, 2H, 2'-H, 5'-H), 6.89 (dd,  $J = 8.4, 1.6$  Hz, 1H, 6'-H), 6.22 (d,  $J = 2.1$  Hz, 1H, 8-H), 6.20 (d,  $J = 2.1$  Hz, 1H, 6-H), 5.49 (dd,  $J = 12.4, 2.8$  Hz, 1H, 2-H), 5.20 (s, 2H, ArOCH<sub>2</sub>), 4.05 (s, 3H, NCH<sub>3</sub>), 3.78 (s, 3H, OCH<sub>3</sub>), 3.27 (dd,  $J = 17.1, 12.5$  Hz, 1H, 3-H), 2.75 (dd,  $J = 17.1, 2.9$  Hz, 1H, 3-H). <sup>13</sup>C NMR (101 MHz, DMSO)  $\delta$  197.33, 166.54, 163.60, 163.19, 148.40, 146.92, 142.34, 131.38, 126.14, 118.23, 114.57, 112.37, 103.24, 95.76, 94.90, 78.93, 62.05, 56.09, 42.59, 36.78; TOF-HRMS:  $m/z$  [M+H]<sup>+</sup>calcd for C<sub>19</sub>H<sub>19</sub>O<sub>6</sub>: 398.1347; found: 398.1340.

**3.1.3.16.** 7-O-((1-ethyl-1H-1,2,3-triazol-4-yl)methyl)hesperetin (**c2**). White crystal, 69% yield, m.p. 195.3–197.6 °C; <sup>1</sup>H NMR (400 MHz, DMSO)  $\delta$  12.12 (s, 1H, 5-OH), 9.14 (s, 1H, 3'-OH), 8.27 (s, 1H, NC=CHN), 6.98–6.93 (m, 2H, 2'-H, 5'-H), 6.90 (dd,  $J = 8.4, 1.9$  Hz, 1H, 6'-H), 6.24 (d,  $J = 2.2$  Hz, 1H, 8-H), 6.21 (d,  $J = 2.2$  Hz, 1H, 6-H), 5.50 (dd,  $J = 12.4, 2.9$  Hz, 1H, 2-H), 5.20 (s, 2H, ArOCH<sub>2</sub>), 4.40 (q,  $J = 7.3$  Hz, 2H, NCH<sub>2</sub>C), 3.78 (s, 3H, OCH<sub>3</sub>), 3.28 (dd,  $J = 17.2, 12.5$  Hz, 1H, 3-H), 2.76 (dd,  $J = 17.1, 3.0$  Hz, 1H, 3-H), 1.44 (t,  $J = 7.3$  Hz, 3H, NCC<sub>2</sub>H<sub>3</sub>). <sup>13</sup>C NMR (101 MHz, DMSO)  $\delta$  197.34, 166.59, 163.61, 163.20, 148.40, 146.93, 142.22, 131.39, 124.77, 118.23, 114.58, 112.38, 103.25, 95.74, 94.88, 78.93, 62.15, 56.10, 45.11, 42.60, 15.83; TOF-HRMS:  $m/z$  [M+H]<sup>+</sup>calcd for C<sub>19</sub>H<sub>19</sub>O<sub>6</sub>: 412.1503; found: 412.1503.

**3.1.3.17.** 7-O-((1-propyl-1H-1,2,3-triazol-4-yl)methyl)hesperetin (**c3**). White crystal, 72% yield, m.p. 206.6–209.2 °C; <sup>1</sup>H NMR (400 MHz, DMSO)  $\delta$  12.12 (s, 1H, 5-OH), 9.15 (s, 1H, 3'-OH), 8.26 (s, 1H, NC=CHN), 6.94 (d,  $J = 8.1$  Hz, 2H, 2'-H, 5'-H), 6.89 (d,  $J = 8.3$  Hz, 1H, 6'-H), 6.23 (d,  $J = 1.9$  Hz, 1H, 8-H), 6.20 (d,  $J = 2.0$  Hz, 1H, 6-H), 5.49 (dd,  $J = 12.4, 2.6$  Hz, 1H, 2-H), 5.20 (s, 2H, ArOCH<sub>2</sub>), 4.33 (t,  $J = 7.0$  Hz, 2H, NCH<sub>2</sub>), 3.78 (s, 3H, OCH<sub>3</sub>), 3.28 (dd,  $J = 17.1, 12.6$  Hz, 1H, 3-H), 2.75 (dd,  $J = 17.1, 2.8$  Hz, 1H, 3-H), 1.83 (h,  $J = 7.2$  Hz, 2H, NCC<sub>2</sub>H<sub>2</sub>C), 0.84 (t,  $J = 7.4$  Hz, 3H, NCC<sub>2</sub>H<sub>3</sub>). <sup>13</sup>C NMR (101 MHz, DMSO)  $\delta$  197.35, 166.58, 163.60, 163.19, 148.40, 146.92, 142.16, 131.38, 125.23, 118.23, 114.57, 112.35, 103.24, 95.75, 94.88, 78.94, 62.14, 56.08, 51.44, 42.60, 23.63, 11.27; TOF-HRMS:  $m/z$  [M+H]<sup>+</sup>calcd for C<sub>19</sub>H<sub>19</sub>O<sub>6</sub>: 426.1660; found: 426.1664.

**3.1.3.18. 7-O-((1-allyl-1H-1,2,3-triazol-4-yl)methyl)hesperetin (c4).** Yellow crystal, 76% yield, m.p. 196.4–198.8 °C;  $^1\text{H}$  NMR (400 MHz, DMSO)  $\delta$  12.11 (s, 1H, 5-OH), 9.14 (s, 1H, 3'-OH), 8.23 (s, 1H, NC=CHN), 6.95 (dd,  $J = 5.1, 3.2$  Hz, 2H, 2'-H, 5'-H), 6.90 (dd,  $J = 8.3, 1.9$  Hz, 1H, 6'-H), 6.23 (d,  $J = 2.2$  Hz, 1H, 8-H), 6.21 (d,  $J = 2.2$  Hz, 1H, 6-H), 6.06 (ddt,  $J = 16.2, 10.3, 5.9$  Hz, 1H, C=CHC-N), 5.50 (dd,  $J = 12.4, 2.9$  Hz, 1H, 2-H), 5.28 (dd,  $J = 10.2, 1.2$  Hz, 1H, CH=CC-N), 5.24–5.15 (m, 3H, CH=CC-N, ArOCH<sub>2</sub>), 5.05 (d,  $J = 5.9$  Hz, 2H, C=CCH<sub>2</sub>N), 3.78 (s, 3H, OCH<sub>3</sub>), 3.28 (dd,  $J = 17.2, 12.5$  Hz, 1H, 3-H), 2.76 (dd,  $J = 17.1, 3.0$  Hz, 1H, 3-H).  $^{13}\text{C}$  NMR (101 MHz, DMSO)  $\delta$  197.35, 166.56, 163.60, 163.20, 148.40, 146.92, 142.41, 133.17, 131.39, 125.35, 119.38, 118.23, 114.58, 112.39, 103.26, 95.75, 94.89, 78.93, 62.06, 56.11, 52.19, 42.60; TOF-HRMS:  $m/z$  [M+H]<sup>+</sup> calcd for C<sub>19</sub>H<sub>19</sub>O<sub>6</sub>: 424.1503; found: 424.1506.

**3.1.3.19. 7-O-((1-butyl-1H-1,2,3-triazol-4-yl)methyl)hesperetin (c5).** White crystal, 79% yield, m.p. 210.7–213.4 °C;  $^1\text{H}$  NMR (400 MHz, DMSO)  $\delta$  12.11 (s, 1H, 5-OH), 9.14 (s, 1H, 3'-OH), 8.26 (s, 1H, NC=CHN), 6.95 (dd,  $J = 5.1, 3.1$  Hz, 2H, 2'-H, 5'-H), 6.90 (dd,  $J = 8.4, 1.9$  Hz, 1H, 6'-H), 6.23 (d,  $J = 2.2$  Hz, 1H, 8-H), 6.21 (d,  $J = 2.2$  Hz, 1H, 6-H), 5.50 (dd,  $J = 12.4, 2.9$  Hz, 1H, 2-H), 5.20 (s, 2H, ArOCH<sub>2</sub>), 4.37 (t,  $J = 7.1$  Hz, 2H, NCH<sub>2</sub>), 3.78 (s, 3H, OCH<sub>3</sub>), 3.28 (dd,  $J = 17.2, 12.5$  Hz, 1H, 3-H), 2.76 (dd,  $J = 17.2, 3.1$  Hz, 1H, 3-H), 1.87–1.71 (m, 2H, NCCCH<sub>2</sub>), 1.31–1.19 (m, 2H, NCCCCH<sub>3</sub>), 0.89 (t,  $J = 7.4$  Hz, 3H, NCCCCH<sub>3</sub>).  $^{13}\text{C}$  NMR (101 MHz, DMSO)  $\delta$  197.34, 166.58, 163.60, 163.20, 148.40, 146.93, 142.17, 131.39, 125.21, 118.22, 114.58, 112.38, 103.25, 95.76, 94.89, 78.94, 62.15, 56.10, 49.57, 42.60, 32.16, 19.54, 13.75; TOF-HRMS:  $m/z$  [M+H]<sup>+</sup> calcd for C<sub>19</sub>H<sub>19</sub>O<sub>6</sub>: 440.1816; found: 440.1814.

**3.1.3.20. 7-O-((1-(cyclopropylmethyl)-1H-1,2,3-triazol-4-yl)methyl)hesperetin (c6).** White crystal, 75% yield, m.p. 208.1–210.3 °C;  $^1\text{H}$  NMR (400 MHz, DMSO)  $\delta$  12.11 (s, 1H, 5-OH), 9.14 (s, 1H, 3'-OH), 8.30 (s, 1H, NC=CHN), 6.95 (dd,  $J = 5.1, 3.2$  Hz, 2H, 2'-H, 5'-H), 6.90 (dd,  $J = 8.4, 1.9$  Hz, 1H, 6'-H), 6.24 (d,  $J = 2.2$  Hz, 1H, 8-H), 6.22 (d,  $J = 2.2$  Hz, 1H, 6-H), 5.50 (dd,  $J = 12.4, 2.9$  Hz, 1H, 2-H), 5.21 (s, 2H, ArOCH<sub>2</sub>), 4.25 (d,  $J = 7.3$  Hz, 2H, NCH<sub>2</sub>), 3.78 (s, 3H, OCH<sub>3</sub>), 3.28 (dd,  $J = 17.2, 12.5$  Hz, 1H, 3-H), 2.76 (dd,  $J = 17.2, 3.1$  Hz, 1H, 3-H), 1.33–1.24 (m, 1H, NCHCH<sub>2</sub>), 0.60–0.53 (m, 2H, CH<sub>2</sub>), 0.46–0.39 (m, 2H, CH<sub>2</sub>).  $^{13}\text{C}$  NMR (101 MHz, DMSO)  $\delta$  197.35, 166.60, 163.60, 163.20, 148.40, 146.93, 142.17, 131.39, 124.97, 118.22, 114.58, 112.39, 103.25, 95.75, 94.88, 78.93, 62.14, 56.11, 54.27, 42.60, 11.83, 4.21, 4.21; TOF-HRMS:  $m/z$  [M+H]<sup>+</sup> calcd for C<sub>19</sub>H<sub>19</sub>O<sub>6</sub>: 438.1660; found: 438.1654.

**3.1.3.21. 7-O-((1-cyclobutyl-1H-1,2,3-triazol-4-yl)methyl)hesperetin (c7).** White crystal, 70% yield, m.p. 199.4–201.8 °C;  $^1\text{H}$  NMR (400 MHz, DMSO)  $\delta$  12.12 (s, 1H, 5-OH), 9.14 (s, 1H, 3'-OH), 8.39 (s, 1H, NC=CHN), 6.98–6.92 (m, 2H, 2'-H, 5'-H), 6.90 (dd,  $J = 8.3, 1.8$  Hz, 1H, 6'-H), 6.24 (d,  $J = 2.2$  Hz, 1H, 8-H), 6.21 (d,  $J = 2.2$  Hz, 1H, 6-H), 5.50 (dd,  $J = 12.4, 2.9$  Hz, 1H, 2-H), 5.20 (s, 2H, ArOCH<sub>2</sub>), 5.14 (dt,  $J = 16.8, 8.5$  Hz, 1H, NCH), 3.78 (s, 3H, OCH<sub>3</sub>), 3.28 (dd,  $J = 17.2, 12.5$  Hz, 1H, 3-H), 2.76 (dd,  $J = 17.1, 3.0$  Hz, 1H, 3-H), 2.53–2.44 (m, 4H, NC(CH<sub>2</sub>)<sub>2</sub>), 1.93–1.79 (m, 2H, CH<sub>2</sub>).  $^{13}\text{C}$  NMR (101 MHz, DMSO)  $\delta$  197.34, 166.57, 163.61, 163.20, 148.41, 146.93, 142.26, 131.39, 123.95, 118.23, 114.57, 112.38, 103.26, 95.73, 94.87, 78.94, 62.16, 56.10, 53.64, 42.60, 30.70, 30.70, 14.86; TOF-HRMS:  $m/z$  [M+H]<sup>+</sup> calcd for C<sub>19</sub>H<sub>19</sub>O<sub>6</sub>: 438.1660; found: 438.1657.

**3.1.3.22. 7-O-((1-cyclopentyl-1H-1,2,3-triazol-4-yl)methyl)hesperetin (c8).** White crystal, 80% yield, m.p. 207.2–210.8 °C;  $^1\text{H}$  NMR (400 MHz, DMSO)  $\delta$  12.11 (s, 1H, 5-OH), 9.14 (s, 1H, 3'-OH), 8.31 (s, 1H, NC=CHN), 6.97–6.92 (m, 2H, 2'-H, 5'-H), 6.89 (dd,  $J = 8.4, 1.7$  Hz, 1H, 6'-H), 6.24 (d,  $J = 2.2$  Hz, 1H, 8-H), 6.21 (d,  $J = 2.2$  Hz, 1H, 6-H), 5.49 (dd,  $J = 12.4, 2.8$  Hz, 1H, 2-H), 5.17 (s, 2H, ArOCH<sub>2</sub>), 4.98

(p,  $J = 6.9$  Hz, 1H, NCH), 3.78 (s, 3H, OCH<sub>3</sub>), 3.28 (dd,  $J = 17.2, 12.5$  Hz, 1H, 3-H), 2.75 (dd,  $J = 17.1, 3.0$  Hz, 1H, 3-H), 2.24–2.12 (m, 2H, CH<sub>2</sub>), 1.94 (td,  $J = 14.1, 6.8$  Hz, 2H, CH<sub>2</sub>), 1.86–1.74 (m, 2H, CH<sub>2</sub>), 1.74–1.61 (m, 2H, CH<sub>2</sub>).  $^{13}\text{C}$  NMR (101 MHz, DMSO)  $\delta$  197.35, 166.61, 163.61, 163.20, 148.40, 146.92, 142.10, 131.38, 124.12, 118.22, 114.57, 112.36, 103.25, 95.72, 94.86, 78.94, 62.18, 61.53, 56.09, 42.60, 33.30, 33.30, 24.06, 24.06; TOF-HRMS:  $m/z$  [M+H]<sup>+</sup> calcd for C<sub>19</sub>H<sub>19</sub>O<sub>6</sub>: 452.1816; found: 452.1815.

**3.1.3.23. 7-O-((1-cyclohexyl-1H-1,2,3-triazol-4-yl)methyl)hesperetin (c9).** White crystal, 82% yield, m.p. 216.3–220.2 °C;  $^1\text{H}$  NMR (400 MHz, DMSO)  $\delta$  12.12 (s, 1H, 5-OH), 9.14 (s, 1H, 3'-OH), 8.31 (s, 1H, NC=CHN), 6.98–6.92 (m, 2H, 2'-H, 5'-H), 6.90 (dd,  $J = 8.3, 1.7$  Hz, 1H, 6'-H), 6.24 (d,  $J = 2.1$  Hz, 1H, 8-H), 6.22 (d,  $J = 2.1$  Hz, 1H, 6-H), 5.50 (dd,  $J = 12.4, 2.8$  Hz, 1H, 2-H), 5.18 (s, 2H, ArOCH<sub>2</sub>), 4.49 (tt,  $J = 11.2, 3.5$  Hz, 1H, NCH), 3.78 (s, 3H, OCH<sub>3</sub>), 3.28 (dd,  $J = 17.1, 12.5$  Hz, 1H, 3-H), 2.76 (dd,  $J = 17.1, 3.0$  Hz, 1H, 3-H), 2.06 (d,  $J = 11.8$  Hz, 2H, CH<sub>2</sub>), 1.87–1.70 (m, 4H, CH<sub>2</sub>, CH<sub>2</sub>), 1.67 (d,  $J = 12.7$  Hz, 1H, CH), 1.49–1.35 (m, 2H, CH<sub>2</sub>), 1.30–1.21 (m, 1H, CH).  $^{13}\text{C}$  NMR (101 MHz, DMSO)  $\delta$  197.34, 166.63, 163.61, 163.20, 148.40, 146.93, 141.87, 131.39, 123.44, 118.21, 114.57, 112.38, 103.25, 95.71, 94.85, 78.94, 62.22, 59.57, 56.10, 42.61, 33.29, 33.29, 25.12, 25.06, 25.06; TOF-HRMS:  $m/z$  [M+H]<sup>+</sup> calcd for C<sub>19</sub>H<sub>19</sub>O<sub>6</sub>: 466.1973; found: 466.1969.

**3.1.3.24. 7-O-((1-(2-hydroxyethyl)-1H-1,2,3-triazol-4-yl)methyl)hesperetin (c10).** White powder, 39% yield, m.p. 236.5–239.9 °C;  $^1\text{H}$  NMR (400 MHz, DMSO)  $\delta$  12.12 (s, 1H, 5-OH), 9.15 (s, 1H, 3'-OH), 8.22 (s, 1H, NC=CHN), 6.94 (d,  $J = 7.5$  Hz, 2H, 2'-H, 5'-H), 6.89 (d,  $J = 8.3$  Hz, 1H, 6'-H), 6.24 (brs, 1H, 8-H), 6.22 (brs, 1H, 6-H), 5.49 (dd,  $J = 12.3, 2.1$  Hz, 1H, 2-H), 5.20 (s, 2H, ArOCH<sub>2</sub>), 5.08 (t,  $J = 5.0$  Hz, 1H, NCC-OH), 4.42 (t,  $J = 5.1$  Hz, 2H, NCH<sub>2</sub>C), 3.78 (s, 5H, OCH<sub>3</sub>, NCCCH<sub>2</sub>O), 3.28 (dd,  $J = 17.1, 12.6$  Hz, 1H, 3-H), 2.75 (dd,  $J = 17.0, 2.3$  Hz, 1H, 3-H).  $^{13}\text{C}$  NMR (101 MHz, DMSO)  $\delta$  197.36, 166.62, 163.61, 163.20, 148.39, 146.91, 141.94, 131.38, 125.86, 118.24, 114.57, 112.35, 103.24, 95.73, 94.88, 78.94, 62.10, 60.26, 56.08, 52.72, 42.60; TOF-HRMS:  $m/z$  [M+H]<sup>+</sup> calcd for C<sub>19</sub>H<sub>19</sub>O<sub>6</sub>: 428.1452; found: 428.1460.

**3.1.3.25. 7-O-((1-(3-hydroxypropyl)-1H-1,2,3-triazol-4-yl)methyl)hesperetin (c11).** White powder, 43% yield, m.p. 219.7–223.3 °C;  $^1\text{H}$  NMR (400 MHz, DMSO)  $\delta$  12.11 (s, 1H, 5-OH), 9.14 (s, 1H, 3'-OH), 8.25 (s, 1H, NC=CHN), 6.94 (d,  $J = 7.7$  Hz, 2H, 2'-H, 5'-H), 6.89 (d,  $J = 8.2$  Hz, 1H, 6'-H), 6.23 (s, 1H, 8-H), 6.21 (s, 1H, 6-H), 5.49 (d,  $J = 11.0$  Hz, 1H, 2-H), 5.20 (s, 2H, ArOCH<sub>2</sub>), 4.70 (t,  $J = 4.7$  Hz, 1H, NCCC-OH), 4.43 (t,  $J = 7.0$  Hz, 2H, NCH<sub>2</sub>), 3.78 (s, 3H, OCH<sub>3</sub>), 3.41 (dd,  $J = 10.6, 5.2$  Hz, 2H, NCCCH<sub>2</sub>O), 3.28 (dd,  $J = 16.9, 12.8$  Hz, 1H, 3-H), 2.76 (d,  $J = 15.4$  Hz, 1H, 3-H), 2.03–1.91 (m, 2H, NCCCH<sub>2</sub>O).  $^{13}\text{C}$  NMR (101 MHz, DMSO)  $\delta$  197.34, 166.58, 163.61, 163.19, 148.40, 146.92, 142.14, 131.38, 125.39, 118.23, 114.58, 112.36, 103.25, 95.74, 94.89, 78.94, 62.13, 57.89, 56.09, 47.19, 42.60, 33.37; TOF-HRMS:  $m/z$  [M+H]<sup>+</sup> calcd for C<sub>19</sub>H<sub>19</sub>O<sub>6</sub>: 442.1609; found: 442.1607.

#### 3.1.4. General procedure for the synthesis of b1-b5

To a solution of acetophenone (3 mmol) in CHCl<sub>3</sub> were added p-TsOH·H<sub>2</sub>O (100 mg, 0.53 mmol) and N-bromosuccinimide (NBS, 214 mg, 3.6 mmol). The mixture was stirred at room temperature for 24 h. The aqueous mixture was extracted with ether (50 mL). The organic layer was dried (Na<sub>2</sub>SO<sub>4</sub>), after filtration, and concentrated under reduced pressure. The residue was purified by silica gel column chromatography (Petroleum ether and CH<sub>2</sub>Cl<sub>2</sub>, 2:1) to obtain white solid. To a solution of the white solid in DMF (50 mL), NaN<sub>3</sub> (143 mg, 2.2 mmol) was added. After stirred at r.t for 3 h, the solid was disappeared completely. Added ascorbic acid (528 mg, 3 mmol) and anhydrous K<sub>2</sub>CO<sub>3</sub> (414 mg, 3 mmol) into the reaction solution, stirred at r.t for 30 min. Then added the intermediate 2

(680 mg, 2 mmol) and  $\text{CuSO}_4 \cdot 5\text{H}_2\text{O}$  (625 mg, 2.5 mmol) into the reaction solution, stirred at r.t for 3 h. Method as described in 4.1.2.2 (acidified to pH 5–6 and extracted with EtOAc, washed with brine solution, dried over anhydrous  $\text{Na}_2\text{SO}_4$ , filtered, and concentrated). The residues of **b1**–**b5**, were purified by flash column chromatography ( $\text{CHCl}_3/\text{Petroleum ether}/\text{methanol} = 1/1, \text{v/v}$ ) [30] (white crystal or powder, yield 36–80% for this step reaction, Scheme 1).

**3.1.4.1. 7-O-((1-(2-oxo-2-phenylethyl)-1H-1,2,3-triazol-4-yl)methyl) hesperetin (b1).** White powder, 61% yield, m.p. 241.1–245.9 °C;  $^1\text{H}$  NMR (400 MHz, DMSO)  $\delta$  12.13 (s, 1H, 5-OH), 9.15 (s, 1H, 3'-OH), 8.24 (s, 1H, NC=CHN), 8.08 (d,  $J = 7.6$  Hz, 2H, ArH), 7.74 (t,  $J = 7.2$  Hz, 1H, ArH), 7.62 (t,  $J = 7.5$  Hz, 2H, ArH), 6.95 (d,  $J = 8.2$  Hz, 2H, 2'-H, 5'-H), 6.90 (d,  $J = 8.2$  Hz, 1H, 6'-H), 6.25 (d,  $J = 13.3$  Hz, 4H, 6-H, 8-H, ArC=OCH<sub>2</sub>N), 5.50 (d,  $J = 11.1$  Hz, 1H, 2-H), 5.28 (s, 2H, ArOCH<sub>2</sub>), 3.78 (s, 3H, OCH<sub>3</sub>), 3.29 (dd,  $J = 16.9, 12.8$  Hz, 1H, 3-H), 2.76 (d,  $J = 16.4$  Hz, 1H, 3-H).  $^{13}\text{C}$  NMR (101 MHz, DMSO)  $\delta$  197.37, 192.61, 166.61, 163.63, 163.22, 148.40, 146.92, 142.19, 134.74, 134.53, 131.39, 129.47, 129.47, 128.66, 128.66, 127.14, 118.24, 114.58, 112.37, 103.27, 95.78, 94.92, 78.95, 62.08, 56.42, 56.09, 42.62; TOF-HRMS:  $m/z$  [M+H]<sup>+</sup> calcd for  $\text{C}_{19}\text{H}_{19}\text{O}_6$ : 502.1609; found: 502.1603.

**3.1.4.2. 7-O-((1-(2-(2-fluorophenyl)-2-oxoethyl)-1H-1,2,3-triazol-4-yl)methyl) hesperetin (b2).** White powder, 53% yield, m.p. 232.4–235.8 °C;  $^1\text{H}$  NMR (400 MHz, DMSO)  $\delta$  12.13 (s, 1H, 5-OH), 9.15 (s, 1H, 3'-OH), 8.22 (s, 1H, NC=CHN), 7.97 (t,  $J = 7.1$  Hz, 1H, ArH), 7.78 (dd,  $J = 13.0, 6.2$  Hz, 1H, ArH), 7.45 (dt,  $J = 15.0, 8.1$  Hz, 2H, ArH), 6.95 (d,  $J = 8.1$  Hz, 2H, 5'-H, 6'-H), 6.90 (d,  $J = 8.2$  Hz, 1H, 2'-H), 6.27 (d,  $J = 1.6$  Hz, 1H, 8-H), 6.24 (d,  $J = 1.6$  Hz, 1H, 6-H), 6.05 (d,  $J = 2.0$  Hz, 2H, ArC=OCH<sub>2</sub>N), 5.50 (dd,  $J = 12.4, 2.5$  Hz, 1H, 2-H), 5.28 (s, 2H, ArOCH<sub>2</sub>), 3.78 (s, 3H, OCH<sub>3</sub>), 3.28 (dd,  $J = 17.1, 12.6$  Hz, 1H, 3-H), 2.76 (dd,  $J = 17.1, 2.7$  Hz, 1H, 3-H).  $^{13}\text{C}$  NMR (101 MHz, DMSO)  $\delta$  197.36, 190.36 ( $^3J = 4.4$  Hz), 166.61, 163.63, 163.22, 162.10 ( $^1J = 255.2$  Hz), 148.41, 146.93, 142.14, 136.85 ( $^3J = 9.1$  Hz), 131.39, 130.85 ( $^4J = 1.8$  Hz), 127.08, 125.58 ( $^3J = 3.1$  Hz), 122.94 ( $^2J = 12.9$  Hz), 118.24, 117.54 ( $^2J = 23.0$  Hz), 114.58, 112.38, 103.27, 95.78, 94.92, 78.95, 62.06, 59.06 ( $^4J = 11.0$  Hz), 56.10, 42.61; TOF-HRMS:  $m/z$  [M+H]<sup>+</sup> calcd for  $\text{C}_{19}\text{H}_{19}\text{O}_6$ : 520.1515; found: 520.1510.

**3.1.4.3. 7-O-((1-(2-(2-chlorophenyl)-2-oxoethyl)-1H-1,2,3-triazol-4-yl)methyl) hesperetin (b3).** White powder, 58% yield, m.p. 229.3–232.6 °C;  $^1\text{H}$  NMR (400 MHz, DMSO)  $\delta$  12.13 (s, 1H, 5-OH), 9.14 (s, 1H, 3'-OH), 8.26 (s, 1H, NC=CHN), 7.99 (d,  $J = 7.6$  Hz, 1H, 1H, ArH), 7.63 (d,  $J = 3.7$  Hz, 2H, ArH), 7.55 (td,  $J = 8.3, 4.3$  Hz, 1H, ArH), 6.95 (d,  $J = 8.0$  Hz, 2H, 5'-H, 6'-H), 6.90 (d,  $J = 8.2$  Hz, 1H, 2'-H), 6.26 (brs, 1H, 8-H), 6.24 (brs, 1H, 6-H), 6.10 (s, 2H, ArC=OCH<sub>2</sub>N), 5.57–5.41 (m, 1H, 2-H), 5.28 (s, 2H, ArOCH<sub>2</sub>), 3.78 (s, 3H, OCH<sub>3</sub>), 3.29 (dd,  $J = 17.0, 12.6$  Hz, 1H, 3-H), 2.76 (dd,  $J = 16.9, 2.2$  Hz, 1H, 3-H).  $^{13}\text{C}$  NMR (101 MHz, DMSO)  $\delta$  197.37, 194.05, 166.59, 163.63, 163.22, 148.41, 146.93, 142.28, 135.01, 134.07, 131.51, 131.39, 131.24, 130.66, 127.98, 127.03, 118.24, 114.58, 112.38, 103.28, 95.78, 94.92, 78.95, 62.01, 58.25, 56.10, 42.62; TOF-HRMS:  $m/z$  [M+H]<sup>+</sup> calcd for  $\text{C}_{19}\text{H}_{19}\text{O}_6$ : 536.1219; found: 536.1217.

**3.1.4.4. 7-O-((1-(2-(2-methoxyphenyl)-2-oxoethyl)-1H-1,2,3-triazol-4-yl)methyl) hesperetin (b4).** White crystal, 60% yield, m.p. 236.7–241.2 °C;  $^1\text{H}$  NMR (400 MHz, DMSO)  $\delta$  12.13 (s, 1H, 5-OH), 9.16 (s, 1H, 3'-OH), 8.23 (s, 1H, NC=CHN), 7.79 (dd,  $J = 7.7, 1.3$  Hz, 1H, ArH), 7.70–7.64 (m, 1H, ArH), 7.28 (d,  $J = 8.4$  Hz, 1H, ArH), 7.11 (t,  $J = 7.5$  Hz, 1H, ArH), 6.95 (d,  $J = 8.4$  Hz, 2H, 2'-H, 5'-H), 6.90 (d,  $J = 8.3$  Hz, 1H, 6'-H), 6.26 (d,  $J = 1.9$  Hz, 1H, 8-H), 6.24 (d,  $J = 1.9$  Hz, 1H, 6-H), 5.94 (s, 2H, ArC=OCH<sub>2</sub>N), 5.50 (dd,  $J = 12.4, 2.6$  Hz, 1H, 2-H), 5.26 (s, 2H, ArOCH<sub>2</sub>), 3.99 (s, 3H, OCH<sub>3</sub>), 3.78 (s, 3H, OCH<sub>3</sub>), 3.28 (dd,  $J = 17.1, 12.6$  Hz, 1H, 3-H), 2.76 (dd,  $J = 17.1, 2.7$  Hz, 1H, 3-H).  $^{13}\text{C}$  NMR (101 MHz, DMSO)  $\delta$  197.36, 192.61, 166.62, 163.62, 163.21,

160.00, 148.40, 146.92, 142.01, 136.09, 131.39, 130.69, 127.10, 124.30, 121.27, 118.23, 114.57, 113.31, 112.36, 103.25, 95.78, 94.92, 78.95, 62.10, 59.96, 56.54, 56.09, 42.62; TOF-HRMS:  $m/z$  [M+H]<sup>+</sup> calcd for  $\text{C}_{19}\text{H}_{19}\text{O}_6$ : 532.1714; found: 532.1714.

**3.1.4.5. 7-O-((1-(2-(4-fluorophenyl)-2-oxoethyl)-1H-1,2,3-triazol-4-yl)methyl) hesperetin (b5).** White powder, 47% yield, m.p. 246.2–248.9 °C;  $^1\text{H}$  NMR (400 MHz, DMSO)  $\delta$  12.13 (s, 1H, 5-OH), 9.16 (s, 1H, 3'-OH), 8.23 (s, 1H, NC=CHN), 8.17 (dd,  $J = 8.3, 5.6$  Hz, 2H, ArH), 7.46 (t,  $J = 8.7$  Hz, 2H, ArH), 6.95 (d,  $J = 8.4$  Hz, 2H, 2'-H, 5'-H), 6.90 (d,  $J = 8.3$  Hz, 1H, 6'-H), 6.27 (d,  $J = 1.6$  Hz, 1H, 8-H), 6.24 (d,  $J = 2.1$  Hz, 1H, 6-H), 6.23 (s, 2H, ArC=OCH<sub>2</sub>N), 5.50 (dd,  $J = 12.4, 2.4$  Hz, 1H, 2-H), 5.28 (s, 2H, ArOCH<sub>2</sub>), 3.78 (s, 3H, OCH<sub>3</sub>), 3.29 (dd,  $J = 17.1, 12.6$  Hz, 1H, 3-H), 2.76 (dd,  $J = 17.1, 2.5$  Hz, 1H, 3-H).  $^{13}\text{C}$  NMR (101 MHz, DMSO)  $\delta$  197.36, 191.30, 166.60, 166.05 ( $^1J = 253.2$  Hz), 163.63, 163.22, 148.40, 146.92, 142.21, 131.78 ( $^3J = 9.7$  Hz), 131.78 ( $^3J = 9.7$  Hz), 131.39, 131.33 ( $^4J = 2.8$  Hz), 127.13, 118.24, 116.58 ( $^2J = 22.0$  Hz), 116.58 ( $^2J = 22.0$  Hz), 114.58, 112.36, 103.26, 95.78, 94.92, 78.95, 62.06, 56.35, 56.08, 42.62; TOF-HRMS:  $m/z$  [M+H]<sup>+</sup> calcd for  $\text{C}_{19}\text{H}_{19}\text{O}_6$ : 520.1515; found: 520.1513.

### 3.1.5. General procedure for the synthesis of d1–d9

To a solution of bromide (2.2 mmol) in DMF (50 mL),  $\text{NaN}_3$  (143 mg, 2.2 mmol) was added. TLC monitored The reaction. After stirred at r.t for 3 h, the solid was disappeared completely. Added ascorbic acid (528 mg, 3 mmol) and anhydrous  $\text{K}_2\text{CO}_3$  (414 mg, 3 mmol) into the reaction solution stirred at r.t for 30 min. Then added the intermediate **3** (680 mg, 2 mmol) and  $\text{CuSO}_4 \cdot 5\text{H}_2\text{O}$  (625 mg, 2.5 mmol) into the reaction solution, stirred at r.t for 3 h. The Method was described in 4.1.2.2 (acidified to pH 5–6 and extracted with EtOAc, washed with brine solution, dried over anhydrous  $\text{Na}_2\text{SO}_4$ , filtered, and concentrated). The residue was recrystallized from EtOAc to obtain the 4-hydroxyimino-7-O-triazoles **d1–d9** (white crystal or powder, yield 36–80% for this step reaction, Scheme 1).

**3.1.5.1. 4-Hydroxyimino 7-O-((1-(2-benzyl-1H-1,2,3-triazol-4-yl)methyl)hesperetin (d1).** White powder, 81% yield, m.p. 233.4–236.8 °C;  $^1\text{H}$  NMR (400 MHz, DMSO)  $\delta$  11.41 (s, 1H, N–OH), 11.35 (s, 1H, 5-OH), 9.11 (s, 1H, 3'-OH), 8.29 (s, 1H, NC=CHN), 7.40–7.31 (m, 5H, ArH), 6.93 (d,  $J = 7.7$  Hz, 2H, 2'-H, 5'-H), 6.87 (d,  $J = 8.3$  Hz, 1H, 6'-H), 6.18 (brs, 2H, 6-H, 8-H), 5.62 (s, 2H, ArCH<sub>2</sub>N), 5.18–5.02 (m, 3H, 2-H, ArOCH<sub>2</sub>), 3.77 (s, 3H, OCH<sub>3</sub>), 3.29 (dd,  $J = 16.8, 2.5$  Hz, 1H, 3-H), 2.81 (dd,  $J = 17.0, 11.4$  Hz, 1H, 3-H).  $^{13}\text{C}$  NMR (101 MHz, DMSO)  $\delta$  160.99, 159.39, 158.14, 153.36, 148.14, 146.90, 143.12, 136.46, 132.41, 129.25, 129.25, 128.65, 128.46, 128.46, 125.27, 117.90, 114.35, 112.37, 98.97, 96.28, 94.97, 76.22, 61.61, 56.07, 53.31, 29.42; TOF-HRMS:  $m/z$  [M+H]<sup>+</sup> calcd for  $\text{C}_{19}\text{H}_{19}\text{O}_6$ : 489.1769; found: 489.1768.

**3.1.5.2. 4-Hydroxyimino-7-O-((1-(2-methylbenzyl)-1H-1,2,3-triazol-4-yl)methyl) hesperetin (d2).** White powder, 77% yield, m.p. 231.5–234.8 °C;  $^1\text{H}$  NMR (400 MHz, DMSO)  $\delta$  11.45 (s, 1H, N–OH), 11.35 (s, 1H, 5-OH), 9.15 (s, 1H, 3'-OH), 8.19 (s, 1H, NC=CHN), 7.29–7.15 (m, 3H, ArH), 7.09 (d,  $J = 7.4$  Hz, 1H, ArH), 6.93 (d,  $J = 7.5$  Hz, 2H, 2'-H, 5'-H), 6.87 (d,  $J = 8.2$  Hz, 1H, 6'-H), 6.18 (brs, 2H, 6-H, 8-H), 5.62 (s, 2H, ArCH<sub>2</sub>N), 5.19–5.05 (m, 3H, 2-H, ArOCH<sub>2</sub>), 3.77 (s, 3H, OCH<sub>3</sub>), 3.29 (dd,  $J = 17.0, 3.0$  Hz, 1H, 3-H), 2.81 (dd,  $J = 17.0, 11.4$  Hz, 1H, 3-H), 2.31 (s, 3H, ArCH<sub>3</sub>).  $^{13}\text{C}$  NMR (101 MHz, DMSO)  $\delta$  160.96, 159.38, 158.12, 153.34, 148.13, 146.87, 143.00, 136.79, 134.55, 132.38, 130.92, 129.15, 128.84, 126.75, 125.34, 117.92, 114.33, 112.34, 98.95, 96.31, 94.99, 76.22, 61.56, 56.05, 51.42, 29.41, 19.11; TOF-HRMS:  $m/z$  [M+H]<sup>+</sup> calcd for  $\text{C}_{19}\text{H}_{19}\text{O}_6$ : 503.1925; found: 503.1926.

**3.1.5.3. 4-Hydroxyimino-7-O-((1-(2-fluorobenzyl)-1H-1,2,3-triazol-4-yl)methyl) hesperetin (d3).** White powder, 72% yield, m.p. 240.2–243.7 °C;  $^1\text{H}$  NMR (400 MHz, DMSO)  $\delta$  11.42 (s, 1H, N–OH), 11.36 (s, 1H, 5-OH), 9.11 (s, 1H, 3'-OH), 8.28 (s, 1H, NC=CHN), 7.42 (dt,  $J = 7.4, 3.7$  Hz, 1H, ArH), 7.36 (t,  $J = 7.2$  Hz, 1H, ArH), 7.30–7.18 (m, 2H, ArH), 6.93 (d,  $J = 8.1$  Hz, 2H, 2'-H, 5'-H), 6.87 (d,  $J = 8.3$  Hz, 1H, 6'-H), 6.18 (brs, 2H, 6-H, 8-H), 5.69 (s, 2H, ArCH<sub>2</sub>N), 5.15–5.05 (m, 3H, 2-H, ArOCH<sub>2</sub>), 3.78 (s, 3H, OCH<sub>3</sub>), 3.29 (dd,  $J = 17.0, 2.9$  Hz, 1H, 3-H), 2.81 (dd,  $J = 17.1, 11.4$  Hz, 1H, 3-H).  $^{13}\text{C}$  NMR (101 MHz, DMSO)  $\delta$  160.99, 160.56 ( $^1J = 246.7$  Hz), 159.39, 158.14, 153.35, 148.14, 146.89, 143.03, 132.41, 131.28 ( $^3J = 3.6$  Hz), 131.22, 125.44, 125.33 ( $^3J = 3.5$  Hz), 123.27 ( $^2J = 14.7$  Hz), 117.90, 116.12 ( $^2J = 20.8$  Hz), 114.35, 112.37, 98.97, 96.27, 94.97, 76.22, 61.54, 56.07, 47.39 ( $^3J = 3.6$  Hz), 29.42; TOF-HRMS:  $m/z$  [M+H]<sup>+</sup> calcd for C<sub>19</sub>H<sub>19</sub>O<sub>6</sub>: 507.1674; found: 507.1675.

**3.1.5.4. 4-Hydroxyimino-7-O-((1-(2-chlorobenzyl)-1H-1,2,3-triazol-4-yl)methyl) hesperetin (d4).** White powder, 79% yield, m.p. 247.5–251.4 °C;  $^1\text{H}$  NMR (400 MHz, DMSO)  $\delta$  11.41 (s, 1H, N–OH), 11.35 (s, 1H, 5-OH), 9.10 (s, 1H, 3'-OH), 8.27 (s, 1H, NC=CHN), 7.52 (d,  $J = 7.4$  Hz, 1H, ArH), 7.39 (tt,  $J = 13.4, 6.6$  Hz, 2H, ArH), 7.24 (d,  $J = 7.2$  Hz, 1H, ArH), 6.93 (d,  $J = 8.4$  Hz, 2H, 2'-H, 5'-H), 6.87 (d,  $J = 8.3$  Hz, 1H, 6'-H), 6.18 (brs, 2H, 6-H, 8-H), 5.73 (s, 2H, ArCH<sub>2</sub>N), 5.12 (s, 2H, ArOCH<sub>2</sub>), 5.09 (dd,  $J = 11.5, 2.9$  Hz, 1H, 2-H), 3.77 (s, 3H, OCH<sub>3</sub>), 3.29 (dd,  $J = 17.0, 2.9$  Hz, 1H, 3-H), 2.81 (dd,  $J = 17.1, 11.4$  Hz, 1H, 3-H).  $^{13}\text{C}$  NMR (101 MHz, DMSO)  $\delta$  160.97, 159.39, 158.14, 153.35, 148.14, 146.89, 142.96, 133.70, 133.11, 132.40, 130.99, 130.75, 130.12, 128.21, 125.70, 117.90, 114.35, 112.37, 98.97, 96.31, 95.00, 76.22, 61.55, 56.07, 51.09, 29.42; TOF-HRMS:  $m/z$  [M+H]<sup>+</sup> calcd for C<sub>19</sub>H<sub>19</sub>O<sub>6</sub>: 523.1379; found: 523.1379.

**3.1.5.5. 4-Hydroxyimino-7-O-((1-propyl-1H-1,2,3-triazol-4-yl)methyl) hesperetin (d5).** White crystal, 77% yield, m.p. 216.1–218.6 °C;  $^1\text{H}$  NMR (400 MHz, DMSO)  $\delta$  11.41 (s, 1H, N–OH), 11.35 (s, 1H, 5-OH), 9.10 (s, 1H, 3'-OH), 8.23 (s, 1H, NC=CHN), 6.93 (d,  $J = 8.3$  Hz, 2H, 2'-H, 5'-H), 6.87 (d,  $J = 8.3$  Hz, 1H, 6'-H), 6.19 (s, 2H, 6-H, 8-H), 5.15–5.05 (m, 3H, 2-H, ArOCH<sub>2</sub>), 4.33 (t,  $J = 7.0$  Hz, 2H, NCH<sub>2</sub>CC), 3.78 (s, 3H, OCH<sub>3</sub>), 3.29 (dd,  $J = 17.0, 2.9$  Hz, 1H, 3-H), 2.81 (dd,  $J = 17.1, 11.4$  Hz, 1H, 3-H), 1.83 (h,  $J = 7.2$  Hz, 1H, NCCH<sub>2</sub>C), 0.84 (t,  $J = 7.4$  Hz, 1H, NCCCH<sub>3</sub>).  $^{13}\text{C}$  NMR (101 MHz, DMSO)  $\delta$  161.03, 159.39, 158.13, 153.35, 148.13, 146.89, 142.70, 132.41, 124.99, 117.89, 114.35, 112.37, 98.95, 96.27, 94.98, 76.21, 61.70, 56.07, 51.42, 29.41, 23.63, 11.27; TOF-HRMS:  $m/z$  [M+H]<sup>+</sup> calcd for C<sub>19</sub>H<sub>19</sub>O<sub>6</sub>: 441.1769; found: 441.1771.

**3.1.5.6. 4-Hydroxyimino-7-O-((1-ethyl-1H-1,2,3-triazol-4-yl)methyl) hesperetin (d6).** White crystal, 81% yield, m.p. 211.6–213.9 °C;  $^1\text{H}$  NMR (400 MHz, DMSO)  $\delta$  11.41 (s, 1H, N–OH), 11.36 (s, 1H, 5-OH), 9.11 (s, 1H, 3'-OH), 8.24 (s, 1H, NC=CHN), 6.93 (d,  $J = 7.7$  Hz, 2H, 2'-H, 5'-H), 6.87 (d,  $J = 8.3$  Hz, 1H, 6'-H), 6.19 (brs, 2H, 6-H, 8-H), 5.16–5.06 (m, 3H, 2-H, ArOCH<sub>2</sub>), 4.39 (q,  $J = 7.3$  Hz, 2H, NCH<sub>2</sub>C), 3.78 (s, 3H, OCH<sub>3</sub>), 3.30 (dd,  $J = 17.0, 3.0$  Hz, 1H, 3-H), 2.82 (dd,  $J = 17.1, 11.4$  Hz, 1H, 3-H), 1.43 (t,  $J = 7.3$  Hz, 3H, NCCH<sub>3</sub>).  $^{13}\text{C}$  NMR (101 MHz, DMSO)  $\delta$  161.04, 159.40, 158.14, 153.35, 148.13, 146.89, 142.76, 132.41, 124.54, 117.90, 114.35, 112.37, 98.95, 96.25, 94.96, 76.21, 61.69, 56.06, 45.07, 29.41, 15.84; TOF-HRMS:  $m/z$  [M+H]<sup>+</sup> calcd for C<sub>19</sub>H<sub>19</sub>O<sub>6</sub>: 427.1612; found: 427.1606.

**3.1.5.7. 4-Hydroxyimino-7-O-((1-butyl-1H-1,2,3-triazol-4-yl)methyl) hesperetin (d7).** White crystal, 75% yield, m.p. 219.8–222.1 °C;  $^1\text{H}$  NMR (400 MHz, DMSO)  $\delta$  11.41 (s, 1H, N–OH), 11.35 (s, 1H, 5-OH), 9.10 (s, 1H, 3'-OH), 8.23 (s, 1H, NC=CHN), 6.93 (d,  $J = 8.4$  Hz, 2H, 2'-H, 5'-H), 6.87 (d,  $J = 8.3$  Hz, 1H, 6'-H), 6.19 (brs, 2H, 6-H, 8-H), 5.14–5.06 (m, 3H, 2-H, ArOCH<sub>2</sub>), 4.36 (t,  $J = 7.1$  Hz, 2H, NCH<sub>2</sub>), 3.78 (s, 3H, OCH<sub>3</sub>), 3.29 (dd,  $J = 17.0, 3.0$  Hz, 1H, 3-H), 2.81 (dd,  $J = 17.1,$

11.4 Hz, 1H, 3-H), 1.84–1.74 (m, 2H, CH<sub>2</sub>), 1.29–1.19 (m, 2H, CH<sub>2</sub>), 0.89 (t,  $J = 7.4$  Hz, 3H, CH<sub>3</sub>).  $^{13}\text{C}$  NMR (101 MHz, DMSO)  $\delta$  161.02, 159.39, 158.13, 153.34, 148.13, 146.89, 142.70, 132.41, 124.97, 117.89, 114.34, 112.37, 98.95, 96.28, 94.97, 76.22, 61.69, 56.07, 49.54, 32.17, 29.42, 19.54, 13.76; TOF-HRMS:  $m/z$  [M+H]<sup>+</sup> calcd for C<sub>19</sub>H<sub>19</sub>O<sub>6</sub>: 455.1925; found: 455.1919.

**3.1.5.8. 4-hydroxyimino-7-O-((1-(cyclopropylmethyl)-1H-1,2,3-triazol-4-yl)methyl) hesperetin (d8).** White powder, 78% yield, m.p. 217.4–221.2 °C;  $^1\text{H}$  NMR (400 MHz, DMSO)  $\delta$  11.41 (s, 1H, N–OH), 11.36 (s, 1H, 5-OH), 9.11 (s, 1H, 3'-OH), 8.27 (s, 1H, NC=CHN), 6.93 (d,  $J = 8.0$  Hz, 2H, 2'-H, 5'-H), 6.87 (d,  $J = 8.3$  Hz, 1H, 6'-H), 6.20 (s, 2H, 6-H, 8-H), 5.16–5.06 (m, 3H, 2-H, ArOCH<sub>2</sub>), 4.24 (d,  $J = 7.3$  Hz, 2H, NCH<sub>2</sub>C), 3.77 (s, 3H, OCH<sub>3</sub>), 3.29 (dd,  $J = 16.9, 2.7$  Hz, 1H, 3-H), 2.81 (dd,  $J = 17.0, 11.4$  Hz, 1H, 3-H), 1.28 (ddd,  $J = 12.4, 7.8, 4.8$  Hz, 1H, NCC), 0.59–0.52 (m, 2H, NCCCH<sub>2</sub>), 0.46–0.38 (m, 2H, NCCCH<sub>2</sub>).  $^{13}\text{C}$  NMR (101 MHz, DMSO)  $\delta$  161.05, 159.40, 158.14, 153.35, 148.13, 146.89, 142.71, 132.40, 124.73, 117.89, 114.35, 112.36, 98.95, 96.26, 94.96, 76.22, 61.67, 56.06, 54.25, 29.42, 11.85, 4.21, 4.21; TOF-HRMS:  $m/z$  [M+H]<sup>+</sup> calcd for C<sub>19</sub>H<sub>19</sub>O<sub>6</sub>: 453.1769; found: 453.1772.

**3.1.5.9. 4-hydroxyimino-7-O-((1-cyclopentyl-1H-1,2,3-triazol-4-yl)methyl) hesperetin (d9).** White powder, 83% yield, m.p. 222.3–225.9 °C;  $^1\text{H}$  NMR (400 MHz, DMSO)  $\delta$  11.41 (s, 1H, N–OH), 11.35 (s, 1H, 5-OH), 9.10 (s, 1H, 3'-OH), 8.28 (s, 1H, NC=CHN), 6.93 (d,  $J = 8.4$  Hz, 2H, 2'-H, 5'-H), 6.90–6.85 (m, 1H, 6'-H), 6.19 (d,  $J = 1.6$  Hz, 2H, 6-H, 8-H), 5.15–5.04 (m, 3H, 2-H, ArOCH<sub>2</sub>), 4.97 (p,  $J = 6.9$  Hz, 1H, NCH), 3.77 (s, 3H, OCH<sub>3</sub>), 3.29 (dd,  $J = 17.0, 3.1$  Hz, 1H, 3-H), 2.81 (dd,  $J = 17.1, 11.3$  Hz, 1H, 3-H), 2.17 (td,  $J = 12.7, 7.1$  Hz, 2H, CH<sub>2</sub>), 1.95 (td,  $J = 14.0, 7.4$  Hz, 2H, CH<sub>2</sub>), 1.87–1.74 (m, 2H, CH<sub>2</sub>), 1.74–1.61 (m, 2H, CH<sub>2</sub>).  $^{13}\text{C}$  NMR (101 MHz, DMSO)  $\delta$  161.06, 159.39, 158.14, 153.34, 148.13, 146.89, 142.63, 132.41, 123.88, 117.89, 114.35, 112.37, 98.95, 96.23, 94.93, 76.21, 61.71, 61.49, 56.07, 33.31, 33.31, 29.42, 24.06, 24.06; TOF-HRMS:  $m/z$  [M+H]<sup>+</sup> calcd for C<sub>19</sub>H<sub>19</sub>O<sub>6</sub>: 467.1925; found: 467.1927.

## 3.2. Biological assay

### 3.2.1. Animal and treatment

C57BL/6j mice (18 g–22 g) were provided by the Experimental Animal Center of Anhui Medical University. Animal experiments and procedures were approved by the Ethics Committee and Animal Experiment Committee of Anhui Medical University.

C57BL/6j mice were randomly divided into six groups, with eight mice in each group. They are the control group, CCl<sub>4</sub> group, different concentrations of compound **d5** treatment group, and silymarin group. Different concentrations of the compound **d5** (50 mg/kg, 100 mg/kg, 200 mg/kg) dissolved in sodium carboxymethylcellulose and silymarin (200 mg/kg) were continuously administered for one week. The control group was given the same concentration of carboxymethylcellulose. In the model group, seven days later, different concentrations of compound **d5** and silymarin treatment group were intraperitoneally and injected with 1% CCl<sub>4</sub> dissolved olive oil to induce an acute liver injury model. The control group was intraperitoneally injected with the same volume of olive oil. After 24 h, the mouse serum was collected and stored in –80 °C for the detection of serological markers. The largest leaf of mouse livers was taken in the same position at approximately 1 cm<sup>3</sup> and fixed with paraformaldehyde for more than 24 h and then, it embedded the livers with paraffin. After sectioning, hematoxylin, and eosin (H&E) staining was performed by standard methods, and pathological changes of the liver were observed under a microscope.

### 3.2.2. Cell culture

We obtained the cell lines of RAW264.7 from Cell Bank of Chinese Academy of Sciences (Shanghai, China) and the cell lines were cultured at 37 °C under 5% CO<sub>2</sub> in DMEM (Hyclone, Logan, UT, USA) medium with 10% FBS (BI), 100 IU/mL Streptomycin and penicillin (Beyotime, Shanghai, China).

### 3.2.3. Determination of cell viability

Cell viability and Cytotoxicity were assessed by an MTT assay (Sigma, Shanghai, China). Before the assay, MTT dissolved in phosphate-buffered saline (PBS) to reach a concentration of 5 mg/mL. First of all, Cells were inoculated into ninety-six hole plates, and then cells cultured at 37 °C for a night with a density of  $7.0 \times 10^3$  cells/well, and reached a total volume of 200  $\mu$ L/well. Then, cells treated with 40  $\mu$ M compounds for 24 h and the same concentration of DMSO as the vehicle. Next, MTT was added to the culture medium with 20  $\mu$ L per well and then incubated at 37 °C for another 4 h. Removing The media and adding 150  $\mu$ L of DMSO into the plates and incubating at 37 °C for 30 min. Finally, the cell viability and cytotoxicity were measured using a microplate reader (Synergy HTX, Biotek, Winooski, VT, USA) and calculated by GraphPad Prism 6 (GraphPad, San Diego, CA, USA).

### 3.2.4. Measurement of production of NO levels

NO levels were determined using the Griess reaction (Beyotime, Shanghai, China), to determine the formation of nitrite, for NO has a short half-life and was oxidized to stable nitrite. RAW 264.7 cells were plated at a density of  $2 \times 10^5$  cells per well in a 24-well culture plate and reached a total of 300  $\mu$ L/well. And they were incubated overnight. The next day, the supernatant was discarded, and different concentrations of pre-configured compounds (1.25, 2.5, 5, 10, 20  $\mu$ M) were added to the plate. Then, stimulate with LPS (1 mg/mL) or not for 24 h. Finally, collect the culture supernatant, use Griess reagent to determine the formation of nitrite, take 50  $\mu$ L culture supernatant and 50  $\mu$ L standard (NaNO<sub>2</sub>) of different concentrations (0–100  $\mu$ M) and add them to the 96-well plate in turn. Add 50  $\mu$ L of GriessI and GriessII reagents, immediately read the absorbance at 540 nm with using a microplate reader (Synergy HTX, Biotek, Winooski, VT, USA). The concentrations of NO were calculated from a sodium nitrite standard curve. Unactivated cells (exposed to media alone) were used as a negative control and activated cells as a positive control. NO production inhibitory activity was calculated as inhibition rate (%):

$$\text{inhibition rate (\%)} = \left[ 1 - \frac{\text{sample}_{(\text{NO concentration})} - \text{negative control}_{(\text{NO concentration})}}{\text{positive control}_{(\text{NO concentration})} - \text{negative control}_{(\text{NO concentration})}} \right] \times 100$$

The IC<sub>50</sub> value was calculated by SPSS23 (IBM, Chicago, Illinois, USA) by the inhibition rate of five different concentrations of compounds on NO.

### 3.2.5. Measurement of cytokines

RAW264.7 cells were planted in a 24-well plate at 200,000 cells per well. After the cells adhere to the wall and before LPS (1 mg/mL) stimulation, the experimental group was pretreated with compounds of 10  $\mu$ M concentration for 1 h, and the control group was treated with the same concentration of DMSO solvent as a control treatment. After 22 h of LPS stimulation, the supernatant was collected in the EP tube. The levels of TNF- $\alpha$ , IL-1 $\beta$ , and IL-6 were measured with ELISA kit (Elabscience, Wuhan, China), and the optical density (OD) was measured at 540 nm using a microplate reader (Synergy HTX, Biotek, Winooski, VT, USA). The results were

analyzed using Origin Pro 8 (OriginLab, Northampton, Massachusetts, USA).

### 3.2.6. Reactive oxygen species (ROS) measurement

The kit is detection using the fluorescent probe DCFH-DA. DCFH is produced when DCFH-DA enters the cell. DCFH is oxidized by active oxygen to form a fluorescent substance DCF, and the level of reactive oxygen species in the cells can be known by detecting the fluorescence of DCF. ROS was detected by Reactive Oxygen Detection Kit (Bestbio, Shanghai, China). RAW264.7 cells ( $1.5 \times 10^6$  cells/well) were cultured in a 6-well plate and reached a total volume of 1 mL/well. After overnight, Cell culture supernatants were removed, pre-configured concentrations of compounds were added and the same concentration of DMSO as compound groups was added as a control. One hour later, the cells were stimulated with LPS (1 mL/L) in addition to the negative wells. After 24 h, the supernatant was removed, washed with PBS and incubated with pre-configured DCFH-DA at 37 °C for 20 min. Collected cells and washed them a third time with a serum-free medium. Fluorescence was detected by CytoFLEX (BECKMAN, Fullerton, CA, USA) at 488 nm excitation and 525 nm emission wavelengths.

### 3.2.7. ALT/AST activity assay

Serum alanine aminotransferase (ALT) and aspartate aminotransferase (AST) activity kits (Jiangcheng, Nanjing, Jiangsu) were used to determine the contents of ALT and AST in the extracted mouse serum. ELISA results were measured with a microplate reader Synergy HTX (Biotek, Winooski, VT, USA) at 510 nm and analyzed using Origin Pro 8 (OriginLab, Northampton, Massachusetts, USA).

### 3.2.8. Western blot analysis

RAW264.7 cells ( $1.5 \times 10^6$  cells/well) were cultured in a 6-well plate and reached a total volume of 1 mL/well. After overnight, Cell culture supernatants were removed, pre-configured concentrations of compounds were added, and the same concentration of DMSO as compound groups was added as a control. One hour later, the cells were stimulated with LPS (1 mL/L) in addition to the negative wells. All the remaining proteins were incubated for 24 h, except that P-P65 and P-ikb were incubated for half an hour. With low-temperature operation, a mixture of RIPA lysis buffer (Beyotime, Shanghai, China) and phosphatase inhibitor (Beibokit, Bestbio, Shanghai, China) is configured. Then, cells are collected and lysed using the pre-prepared lysis buffer. After full lysis, the lysate was fully lysed and centrifuged (4 °C, 30 min, 12,000 rpm, Beckman Coulter, Inc., Fullerton, California, USA) to carefully extract the supernatant. The total protein concentration was determined using BCA Protein Assay Kit (Beyotime, Shanghai, China). Boil the sample at 100 °C for 5 min to denature and stabilize the protein. The amount of sample loaded was determined based on the protein quantification results, and fractionated using SDS polyacrylamide gel, and transferred to a polyvinylidene fluoride membrane (PVDF) (Merck Millipore, Tullagreen Carrigtwohill, Ireland). The PVDF membrane was blocked in a TBST solution containing 5% skimmed milk or 3% BSA (Albumin Bovine V, Sigma), and then Incubated the primary antibody overnight at 4 °C:  $\beta$ -actin (1:1000 dilution; Abcam, Cambridge, MA, USA), iNOS (1:1000 dilution; Abcam, Cambridge, MA, USA), COX-2 (1: 1000 dilution; CST, Danvers, MA, USA), NF- $\kappa$ B (1:1000 dilution; CST, Danvers, MA, USA). After the primary antibody was incubated overnight, it was washed 3 times with TBST containing Tween 20. The PVDF membrane was incubated with the secondary antibody for 1 h at room temperature. After washing 3 times, it was developed by an ultra-sensitive

enhanced chemiluminescence (ECL) substrate (ECL-plus, Thermo Scientific, Rockford, IL, USA).

#### 4. Statistical analysis

Data are expressed as the mean  $\pm$  standard deviation (SD) of independently performed experiments and repeated the experiment at least three times. SPSS 23 (IBM, Chicago, IL, USA) was used to analyze the significant difference of the drug blank group, the drug treatment group and the positive control group VS the model group. When  $p(*) < 0.05$ ,  $p(**) < 0.01$ ,  $p(***) < 0.001$ , the difference was considered to be statistically significant.

#### 5. Conclusions

In conclusion, we successfully synthesized **39** new hesperetin 7-O-1, 2, 3-triazole derivatives and evaluated their anti-inflammatory activity. Preliminary evaluation results showed that compared with the positive control and the previous amide series compounds **4d** and **4k**, most of the compounds had more effective inhibition on NO and TNF- $\alpha$ , IL-1 $\beta$ , IL-6 produced by LPS-induced RAW264.7. Among the synthesized compounds, compound **d5** seemed to be the most effective. Besides, compound **d5** inhibited ROS production in a concentration-dependent manner. These results showed that the compound's anti-inflammatory mechanism might be through negative regulation of the NF- $\kappa$ B signaling pathway and to further inhibit the expression of iNOS and COX-2 from inhibit the inflammatory process. The results of in vivo studies showed that in the CCL<sub>4</sub>-induced acute liver injury model, compound **d5** exerted anti-inflammatory effects by inhibiting the expression of cytokines such as TNF- $\alpha$ , IL-1 $\beta$  and IL-6 in the serum and reduced ALT and AST. In conclusion, **d5** showed promising anti-inflammatory activity and may be beneficial in treating ALI-related inflammatory processes.

#### Declaration of competing interest

The authors declare that they have no known competing financial interests or personal relationships that could have appeared to influence the work reported in this paper.

#### Acknowledgments

Thanks to the support of National Natural Science Foundation of China (No. U19A2001); Thank you for the support of the Natural Science Foundation of Anhui Province University (KJ2019A0233); Thanks for the support of The University Synergy Innovation Program of Anhui Province (No. GXXT-2019-045); Thanks to the Center for Scientific Research of Anhui Medical University for valuable help in our experiment.

#### Appendix A. Supplementary data

Supplementary data to this article can be found online at <https://doi.org/10.1016/j.ejmech.2021.113162>.

#### References

- [1] A. Eguchi, A. Wree, A.E. Feldstein, Biomarkers of liver cell death, *J. Hepatol.* 60 (2014) 1063–1074, <https://doi.org/10.1016/j.jhep.2013.12.026>, 2014/01/15.
- [2] J.F. Crismale, S.L. Friedman, Acute liver injury and decompensated cirrhosis, *Med. Clin.* 104 (2020) 647–662, <https://doi.org/10.1016/j.mcna.2020.02.010>, 2020/06/09.
- [3] Chenxia Hu, Lingfei Zhao, Zhongwen Wu, et al., Transplantation of mesenchymal stem cells and their derivatives effectively promotes liver regeneration to attenuate acetaminophen-induced liver injury, *J. Stem Cell Res. Ther.* 11 (2020) 88, <https://doi.org/10.1186/s13287-020-01596-9>.
- [4] R.F. Schwabe, T. Luedde, Apoptosis and necroptosis in the liver: a matter of life and death, *Nat. Rev. Gastroenterol. Hepatol.* 15 (2018) 738–752, <https://doi.org/10.1038/s41575-018-0065-y>.
- [5] B. Bhushan, U. Apte, Liver regeneration after acetaminophen hepatotoxicity: mechanisms and therapeutic opportunities, *Am. J. Pathol.* 189 (2019) 719–729, <https://doi.org/10.1016/j.ajpath.2018.12.006>, 2019/01/18.
- [6] Y.S. Choi, J. Lee, H.W. Lee, et al., Liver injury in acute hepatitis A is associated with decreased frequency of regulatory T cells caused by Fas-mediated apoptosis, *Gut* 64 (2015) 1303–1313, <https://doi.org/10.1136/gutjnl-2013-306213>, 2014/07/11.
- [7] K. Roth, J. Strickland, B.L. Copple, Regulation of macrophage activation in the liver after acute injury: role of the fibrinolytic system, *World J. Gastroenterol.* 26 (2020) 1879–1887, <https://doi.org/10.3748/wjg.v26.i16.1879>, 2020/05/12.
- [8] L.C. Anders, A.L. Lang, A. Anwar-Mohamed, et al., Vinyl chloride metabolites potentiate inflammatory liver injury caused by LPS in mice, *Toxicol. Sci.* 151 (2016) 312–323, <https://doi.org/10.1093/toxsci/kfw045>, 2016/03/11.
- [9] F. Bessone, M. Robles-Diaz, N. Hernandez, et al., Assessment of serious acute and chronic idiosyncratic drug-induced liver injury in clinical practice, *Semin. Liver Dis.* 39 (2019) 381–394, <https://doi.org/10.1055/s-0039-1685519>, 2019/05/03.
- [10] P. Grewal, J. Ahmad, Severe liver injury due to herbal and dietary supplements and the role of liver transplantation, *World J. Gastroenterol.* 25 (2019) 6704–6712, <https://doi.org/10.3748/wjg.v25.i46.6704>, 2019/12/21.
- [11] X. Fan, L. Lin, B. Cui, et al., Therapeutic potential of genipin in various acute liver injury, fulminant hepatitis, NAFLD and other non-cancer liver diseases: more friend than foe, *Pharmacol. Res.* 159 (2020) 104945, <https://doi.org/10.1016/j.phrs.2020.104945>, 2020/05/27.
- [12] M.S. Islam, H. Yu, L. Miao, et al., Hepatoprotective effect of the ethanol extract of illicium henryi against acute liver injury in mice induced by lipopolysaccharide, *Antioxidants* 8 (2019), <https://doi.org/10.3390/antiox8100446>, 2019/10/05.
- [13] D.S. Kim, S.B. Lim, Semi-continuous subcritical water extraction of flavonoids from citrus unshiu peel: their antioxidant and enzyme inhibitory activities, *Antioxidants* 9 (2020), <https://doi.org/10.3390/antiox9050360>, 2020/04/30.
- [14] H. Parhiz, A. Roohbakhsh, F. Soltani, et al., Antioxidant and anti-inflammatory properties of the citrus flavonoids hesperidin and hesperetin: an updated review of their molecular mechanisms and experimental models, *Phytother. Res.* 29 (2015) 323–331, <https://doi.org/10.1002/ptr.5256>.
- [15] S.S. Cho, J.H. Yang, K.H. Seo, et al., Cudrania tricuspidata extract and its major constituents inhibit oxidative stress-induced liver injury, *J. Med. Food* 22 (2019) 602–613, <https://doi.org/10.1089/jmf.2018.4322>, 2019/05/03.
- [16] Jie-Qiong Ma, Yun-Zhi Sun, Qing-Lei Ming, et al., Ampelopsin attenuates carbon tetrachloride-induced mouse liver fibrosis and hepatic stellate cell activation associated with the SIRT1/TGF- $\beta$ 1/Smad3 and autophagy pathway, *Int. Immunopharm.* 77 (2019) 105984, <https://doi.org/10.1016/j.intimp.2019.105984>, undefined.
- [17] H.Yuan Menggensilimu, C. Zhao, et al., Anti-liver fibrosis effect of total flavonoids from Scabiosa comosa Fisch. ex Roem. et Schult. on liver fibrosis in rat models and its proteomics analysis, *Ann. Palliat. Med.* 9 (2020) 272–285, <https://doi.org/10.21037/apm.2020.02.29>, 2020/04/03.
- [18] Y. Li, A.D. Kandhare, A.A. Mukherjee, et al., Acute and sub-chronic oral toxicity studies of hesperidin isolated from orange peel extract in Sprague Dawley rats, *Regul. Toxicol. Pharmacol.* 105 (2019) 77–85, <https://doi.org/10.1016/j.yrtph.2019.04.001>, 2019/04/17.
- [19] L. Dong, L. Yin, H. Quan, et al., Hepatoprotective effects of kaempferol-3-O-alpha-L-Arabinopyranosyl-7-O-alpha-L-Rhamnopyranoside on d-galactosamine and lipopolysaccharide caused hepatic failure in mice, *Molecules* 22 (2017), <https://doi.org/10.3390/molecules22101755>, 2017/10/24.
- [20] J. Vucicevic, K. Nikolic, J.B.O. Mitchell, Rational drug design of antineoplastic agents using 3D-QSAR, cheminformatic, and virtual screening approaches, *Curr. Med. Chem.* 26 (2019) 3874–3889, <https://doi.org/10.2174/0929867324666170712115411>, 2017/07/15.
- [21] Q. Jiao, L. Xu, L. Jiang, et al., Metabolism study of hesperetin and hesperidin in rats by UHPLC-LTQ-Orbitrap MSn, *Xenobiotica* (2019) 1–27, <https://doi.org/10.1080/00498254.2019.1567956>.
- [22] C. Shen, R. Chen, Z. Qian, et al., A HPLC-MS/MS method for the quantitation of free, conjugated, and total HDND-7, a novel hesperetin derivative, in rat plasma and tissues: application to the pharmacokinetic and tissue distribution study, *J. Pharmaceut. Biomed. Anal.* 118 (2016) 149–160, <https://doi.org/10.1016/j.jpba.2015.10.031>, 2015/11/10.
- [23] B. Li, A.L. Huang, Y.L. Zhang, et al., Design, synthesis and evaluation of hesperetin derivatives as potential multifunctional anti-Alzheimer agents, *Molecules* 22 (2017), <https://doi.org/10.3390/molecules22071067>, 2017/07/05.
- [24] H.W. Ding, A.L. Huang, Y.L. Zhang, et al., Design, synthesis and biological evaluation of hesperetin derivatives as potent anti-inflammatory agent, *Fitoterapia* 121 (2017) 212–222, <https://doi.org/10.1016/j.fitote.2017.07.016>, 2017/08/05.
- [25] Y. Zhang, Y. Zheng, W. Shi, et al., Design, synthesis and investigation of the potential anti-inflammatory activity of 7-O-amide hesperetin derivatives, *Molecules* 24 (2019), <https://doi.org/10.3390/molecules24203663>.
- [26] A.-L. Huang, Y.-L. Zhang, H.-W. Ding, et al., Design, synthesis and investigation of potential anti-inflammatory activity of O-alkyl and O-benzyl hesperetin derivatives, *Int. Immunopharm.* 61 (2018) 82–91, <https://doi.org/10.1016/j.intimp.2018.05.009>.
- [27] C. Shen, Z. Qian, R. Chen, et al., Single dose oral and intravenous pharmacokinetics and tissue distribution of a novel hesperetin derivative MTBH in rats,

- Eur. J. Drug Metab. Pharmacokinet. 41 (2015) 675–688, <https://doi.org/10.1007/s13318-015-0293-2>.
- [28] Roxana Martínez-Pascual, Socorro Meza-Reyes, José Luis Vega-Baez, et al., Novel synthesis of steroidal oximes and lactams and their biological evaluation as antiproliferative agents, *Steroids* 122 (2017) 24–33, <https://doi.org/10.1016/j.steroids.2017.03.008>.
- [29] S. Haider, M.S. Alam, H. Hamid, et al., Synthesis of novel 1,2,3-triazole based benzoxazolinones: their TNF- $\alpha$  based molecular docking with in-vivo anti-inflammatory, antinociceptive activities and ulcerogenic risk evaluation, *Eur. J. Med. Chem.* 70 (2013) 579–588, <https://doi.org/10.1016/j.ejmech.2013.10.032>, 2013/11/12.
- [30] M.G. Perrone, P. Vitale, A. Panella, et al., General role of the amino and methylsulfamoyl groups in selective cyclooxygenase(COX)-1 inhibition by 1,4-diaryl-1,2,3-triazoles and validation of a predictive pharmacometric PLS model, *Eur. J. Med. Chem.* 94 (2015) 252–264, <https://doi.org/10.1016/j.ejmech.2015.02.049>, 2015/03/15.
- [31] J. Akhtar, A.A. Khan, Z. Ali, et al., Structure-activity relationship (SAR) study and design strategies of nitrogen-containing heterocyclic moieties for their anticancer activities, *Eur. J. Med. Chem.* 125 (2017) 143–189, <https://doi.org/10.1016/j.ejmech.2016.09.023>, 2016/09/24.
- [32] S.P. Assis, M.T. da Silva, R.N. de Oliveira, et al., Synthesis and anti-inflammatory activity of new alkyl-substituted phthalimide 1H-1,2,3-triazole derivatives, *Sci. World J.* 2012 (2012) 925925, <https://doi.org/10.1100/2012/925925>, 2013/01/11.
- [33] H.B. Zhang, Q.K. Shen, H. Wang, et al., Synthesis and evaluation of novel arctigenin derivatives as potential anti-Toxoplasma gondii agents, *Eur. J. Med. Chem.* 158 (2018) 414–427, <https://doi.org/10.1016/j.ejmech.2018.08.087>, 2018/09/22.
- [34] R. Zeferino-Diaz, L. Olivera-Castillo, A. Davalos, et al., 22-Oxcholestane oximes as potential anti-inflammatory drug candidates, *Eur. J. Med. Chem.* 168 (2019) 78–86, <https://doi.org/10.1016/j.ejmech.2019.02.035>, 2019/02/25.
- [35] K.K. Park, D.H. Ko, Z. You, et al., In vitro anti-inflammatory activities of new steroidal antidrugs: [16 $\alpha$ ,17 $\alpha$ -d] isoxazoline and [16 $\alpha$ ,17 $\alpha$ -d]-3'-hydroxy-iminoformyl isoxazoline derivatives of prednisolone and 9 $\alpha$ -fluoroprednisolone, *Steroids* 71 (2006) 183–188, <https://doi.org/10.1016/j.steroids.2005.10.003>, 2005/11/29.
- [36] M. Correia-da-Silva, E. Sousa, B. Duarte, et al., Flavonoids with an oligopolysulfated moiety: a new class of anticoagulant agents, *J. Med. Chem.* 54 (2011) 95–106, <https://doi.org/10.1021/jm1013117>, 2010/12/09.
- [37] Y. Yang, Z. Wei, A.T. Teichmann, et al., Development of a novel nitric oxide (NO) production inhibitor with potential therapeutic effect on chronic inflammation, *Eur. J. Med. Chem.* 193 (2020) 112216, <https://doi.org/10.1016/j.ejmech.2020.112216>, 2020/03/26.
- [38] X. Chen, H.-W. Ding, H.-D. Li, et al., Hesperetin derivative-14 alleviates inflammation by activating PPAR- $\gamma$  in mice with CCl<sub>4</sub>-induced acute liver injury and LPS-treated RAW264.7 cells, *Toxicol. Lett.* 274 (2017) 51–63, <https://doi.org/10.1016/j.toxlet.2017.04.008>.
- [39] Y.H. Lin, Y.H. Hsiao, K.L. Ng, et al., Physalin A attenuates inflammation through down-regulating c-Jun NH2 kinase phosphorylation/Activator Protein 1 activation and up-regulating the antioxidant activity, *Toxicol. Appl. Pharmacol.* (2020) 115115, <https://doi.org/10.1016/j.taap.2020.115115>, 2020/07/08.
- [40] M. Ramalingam, S.J. Kim, Pharmacological activities and applications of spicatoside A, *Biomol. Ther. (Seoul)* 24 (2016) 469–474, <https://doi.org/10.4062/biomolther.2015.214>, 2016/05/14.
- [41] Tingting Yu, Xingzhen Lao, Heng Zheng, Influencing COX-2 activity by COX related pathways in inflammation and cancer.[J], *Mini Rev. Med. Chem.* 16 (2016) 1230–1243, <https://doi.org/10.2174/13895575166661605051157>.
- [42] R. Sethi, N. Gomez-Coronado, A.J. Walker, et al., Neurobiology and therapeutic potential of cyclooxygenase-2 (COX-2) inhibitors for inflammation in neuro-psychiatric disorders, *Front. Psychiatr.* 10 (2019) 605, <https://doi.org/10.3389/fpsy.2019.00605>, 2019/09/26.
- [43] A. Hilliard, P. Mendonca, K.F.A. Soliman, Involvement of NF $\kappa$ B and MAPK signaling pathways in the preventive effects of Ganoderma lucidum on the inflammation of BV-2 microglial cells induced by LPS, *J. Neuroimmunol.* 345 (2020) 577269, <https://doi.org/10.1016/j.jneuroim.2020.577269>, 2020/06/02.
- [44] W. Wang, Y. Wu, X. Chen, et al., Synthesis of new ent-labdane diterpene derivatives from andrographolide and evaluation of their anti-inflammatory activities, *Eur. J. Med. Chem.* 162 (2019) 70–79, <https://doi.org/10.1016/j.ejmech.2018.11.002>, 2018/11/13.
- [45] L.Z. Chen, W.W. Sun, L. Bo, et al., New arylpyrazoline-coumarins: synthesis and anti-inflammatory activity, *Eur. J. Med. Chem.* 138 (2017) 170–181, <https://doi.org/10.1016/j.ejmech.2017.06.044>, 2017/07/02.
- [46] A. El-Kenawi, B. Ruffell, Inflammation, ROS, and mutagenesis, *Canc. Cell* 32 (2017) 727–729, <https://doi.org/10.1016/j.ccell.2017.11.015>, 2017/12/13.
- [47] O. Leavy, Inflammation: regulating ROS, *Nat. Rev. Immunol.* 14 (2014) 357, <https://doi.org/10.1038/nri3685>, 2014/05/07.
- [48] Y.R. Xue, S. Yao, Q. Liu, et al., Dihydro-stilbene gigantol relieves CCl<sub>4</sub>-induced hepatic oxidative stress and inflammation in mice via inhibiting C5b-9 formation in the liver, *Acta Pharmacol. Sin.* 41 (2020) 1433–1445, <https://doi.org/10.1038/s41401-020-0406-6>, 2020/05/15.
- [49] S. Munakarmi, L. Chand, H.B. Shin, et al., Indole-3-Carbinol derivative DIM mitigates carbon tetrachloride-induced acute liver injury in mice by inhibiting inflammatory response, apoptosis and regulating oxidative stress, *Int. J. Mol. Sci.* 21 (2020), <https://doi.org/10.3390/ijms21062048>, 2020/03/21.
- [50] X. Zhang, G. Kuang, J. Wan, et al., Salidroside protects mice against CCl<sub>4</sub>-induced acute liver injury via down-regulating CYP2E1 expression and inhibiting NLRP3 inflammasome activation, *Int. Immunopharm.* 85 (2020) 106662, <https://doi.org/10.1016/j.intimp.2020.106662>, 2020/06/17.
- [51] M. Wang, J. Niu, L. Ou, et al., Zerumbone protects against carbon tetrachloride (CCl<sub>4</sub>)-induced acute liver injury in mice via inhibiting oxidative stress and the inflammatory response: involving the TLR4/NF- $\kappa$ B/COX-2 pathway, *Molecules* 24 (2019), <https://doi.org/10.3390/molecules24101964>, 2019/05/28.